Master's thesis

NTNU
Norwegian University of Science and Technology
Faculty of Social and Educational Sciences
Department of Psychology

Rikke Ingeborg Henriksen

Identification of the Most Suitable Pheromone and Interspecific Odorant Stimuli in Respect to Their Quantities for the Application in Calcium Imaging on the Moth's Primary Olfactory Center

Master's thesis in Psychology

Supervisor: Elena Ian and Bente G. Berg

May 2020

NTNU
Norwegian University of
Science and Technology

Rikke Ingeborg Henriksen

Identification of the Most Suitable Pheromone and Interspecific Odorant Stimuli in Respect to Their Quantities for the Application in Calcium Imaging on the Moth's Primary Olfactory Center

Master's thesis in Psychology
Supervisor: Elena Ian and Bente G. Berg
May 2020

Norwegian University of Science and Technology
Faculty of Social and Educational Sciences
Department of Psychology

NTNU
Norwegian University of
Science and Technology

Table of Content

Abstract

The calcium imaging technique used in this project allows for the investigation of the second-order projection neurons (PNs) confined to the primary olfactory center of the moth *Helicoverpa armigera* brain. The focus of the study was on a specific area of the AL, the macroglomerular complex (MGC), responsible for the processing of information regarding female produced components. In order to describe the response profile of the MGC PNs, two pheromones and one interspecific component were used as odor stimuli. In previous calcium imaging experiments, including those performed in the Chemosensory lab, quite high concentration stimuli were used, which were hardly close to naturally occurring signals in the moth olfactory environment. The aim of the present study was to identify a more relevant stimulus concentration for the usage in calcium imaging experiments. In order to do so, retrogradely stained medial antennal lobe tract (mALT) PNs were investigated on their activity in response to the concentrations ranging from 10^{-3} to 10^{-8} of two pheromone components, *cis*-11-hexadecenal (Z11-16:Ald) and *cis*-9-hexadecenal (Z9-16:Ald), and one interspecific component, *cis*-9-tetradecenal (Z9-14:Ald). PNs in the MGC units showed high sensitivity to these components and were able to detect relatively low quantities of components in comparison with the previously used stimuli.

The results obtained in this project demonstrate that the previously used concentrations are indeed too high, and the concentration 10^{-4} is suitable enough to elicit strong responses in all the investigated MGC units in the AL. In addition, methodological weaknesses were identified during processing of raw data, where some preparations showed discrepancies between raw data and processed data in KNIME software program.

Acknowledgements

The experimental work presented in this thesis was conducted in the Chemosensory lab under the Department of Psychology at the Norwegian University of Science and Technology.

I would like to give special thanks to my main supervisor Elena Ian for patiently teaching me the experimental procedures and helping me throughout the whole process. Her support and encouragement are highly appreciated. I would also like to thank the head of the Chemosensory lab, my co-supervisor Bente G. Berg, for being engaged in the project and provide valuable input. Next, I would like to thank all the members of the Chemosensory lab for providing a nice and welcoming atmosphere. I appreciate being a part of such a great learning environment. Lastly, I would like to thank my family and friends for supporting and encouraging me though all my years of studying leading up to this thesis.

Abbreviations

OSN – Olfactory sensory neuron

OR – Olfactory receptor

AL – Antennal lobe

MGC – Macroglomerular complex

Cu – Cumulus

DMP – Dorsomedial posterior

DMA – Dorsomedial anterior

ALT – Antennal lobe tract

LN – Local interneuron

PN – Projection neuron

CN – Centrifugal neuron

MB – Mushroom body

LH – Lateral horn

1. Introduction

Centuries back, in the 1870s, a french naturalist named Jean-Henri Fabre found himself fascinated by the ability of the female peacock moth to attract males of the same species. He wondered what made the males so attracted to the female. It was soon concluded that it had to be some kind of female-released chemical substances (Reviewed by Patlak et al., 2003). Decades later, Adolf Butenandt, who was already famous for identifying the human hormones estrogen, testosterone and progesterone, found himself intrigued by the chemical substances produced by female moths. After years of research, he finally identified the female attractant substance of the silk moth *Bombyx mori* in 1959. The signal molecule identified was a kind of alcohol which he named Bombykol (Butenandt, 1959).

After Butenandt's big breakthrough the research field grew, and scientists started to identify pheromones in other species as well. Soon, the focus shifted from studying beneficial insects, like the silk moth and honeybee, to investigation of pestiferous species. Today, pheromones of more than 1600 insects have been identified, and they have shown to be critical in terms of pest management. By using pheromone compounds, one can actually manipulate insect behavior. Farmers started to take advantage of this and used mate disruption as a method to save their crops from pesters. Mate disruption proved to be more effective than insecticides in general and is the preferred method among farmers today (Reviewed by Patlak et al., 2003).

The insect olfactory system has, in addition, over decades gained popularity among researchers as a model system. Honeybees, flies, cockroaches and moths are species widely used as experimental objects due to their easily accessible nervous system. Even though insects are insignificant in the eyes of many people, the reality is that they have a fascinating and complex nervous system, making them great model organisms for research on different sensory systems, including olfaction. Despite their phylogenetic differences, invertebrates and vertebrates have a range of similarities concerning the anatomy and physiology of the olfactory system. This may indicate that the same basic mechanisms govern the chemosensory pathways in both groups. What makes the insects highly valuable to researchers is the possibility to investigate these mechanisms in well-defined neural circuits that are accessible for suitable experiments.

The cotton bollworm moth species, *Helicoverpa armigera*, is known worldwide as a serious crop damaging pest. It is one of the 365 species within the Heliothinae (Lepidoptera:

Noctuidae) subfamily, including some of the most extensively studied moths (Reviewed by Berg et al., 2014). Males of *H. armigera* were used as experimental organisms in this project. What makes this subfamily especially interesting is the pheromone communication system that prevails not only within the different species but also across the species. This will be further discussed in the following section.

In this study, an experimental approach implying calcium imaging measurements of odor-evoked responses from the moth brain was taken. The main aim was to identify the most relevant stimulus concentrations for pheromone signal detection. Various concentrations of two species-specific pheromones and one interspecific component were used as stimuli to elicit responses in the male-specific macroglomerular complex (MGC) in the antennal lobe (AL). The strength of the responses was then plotted in a dose-response curve. Both interspecific and conspecific components elicited strong neuronal responses but in different subareas of the MGC. The calcium imaging technique allowed identification of the MGC units and their distinct activation during stimulus application.

1.1 Pheromones and Interspecific Signals

Throughout the time, several definitions have been proposed for what we collectively term "pheromones" today. Karlson and Luscher (1959) were the first ones to introduce the biological term and defined it as: "*Substances which are secreted to the outside by an individual and received by a second individual of the same species, in which they release a specific behavioral reaction*". In moths, these substances allow for sexual interaction between males and females within the same species. Female moths secrete sex pheromones and males detect them, often over long distances. The moth olfactory system is sexually dimorphic, where males have additional structures within the AL dedicated to pheromone detection. Interestingly, the typical sex pheromone in moths is a blend of several compounds (Reviewed by Berg et al., 2014). The blend composition differs among distinct species. Many of the heliothine moths studied utilize similar key components in their pheromone blend, but in different ratios. For example, *H. armigera* uses the same two compounds as essential sex pheromones as the sympatric species, *Helicoverpa assulta*. However, the two-component blends of the species have almost opposite ratios – 100:2 and 6:100, respectively (Chang et al., 2016). Generally, males are attracted to components secreted by conspecific females,

while components elicited by heterospecific females may inhibit attraction (Mustaparta, 1996). This clever system maintains the distinct species and prevents mating across species.

In a study conducted by Zhang et al. (2012), a total of ten compounds were identified in the female sex gland of *H. armigera*. Nevertheless, according to a behavioral long distance study only two of them, the primary pheromone *cis*-11-hexadenal (Z11-16:Ald) and the secondary pheromone *cis*-9-hexadenal (Z9-16:Ald), comprising a binary blend, turned out to be necessary and sufficient to elicit the sexual response in males (Kehat et al., 1980). Since several heliothine species use the same major component, the presence of a secondary pheromone constituent is crucial for establishing species-specific blends. In addition, the interspecific components serve an important role in sustaining the species diversity. In *H. armigera,* two components, *cis*-9-tetradecenal (Z9-14:Ald) and *cis*-11-hexadecenol (Z11-16:OH) play a role as interspecific signal molecules, acting as behavioral antagonists (Reviewed by Berg et al., 2014). Intriguingly, however, Z9-14:Ald seems to fill a dual role – depending on concentration. Adding lower quantities of this compound to the main pheromone blend actually increases male attraction, while the inhibitory effect is induced by higher quantities (Wu et al., 2015). This implies that behavioral responses of males are highly dependent on the component concentration within a blend.

1.2 Peripheral Organization of the Moth Olfactory System

The moth antennae are equipped with sensilla, which are hair-like structures containing olfactory sensory neurons (OSNs). During odorant exposure, airborne molecules enter the sensillum lymph through pores in the sensilla. Once inside, the ligand is transported to the OSN via specific proteins. Generally, plant volatiles are transported by odorant-binding proteins, while pheromones are carried by pheromone-binding proteins. OSNs express two main classes of odor receptors: olfactory receptors (ORs) detecting plant odors, and male-specific pheromone receptors detecting pheromones (Reviewed by Zhang & Löfstedt, 2015). Each OSN expresses only one type of olfactory receptor, and all OSNs expressing identical olfactory receptor types project to the same AL glomerulus (Hallem & Carlson, 2006).

ORs detecting pheromones obtain the same seven-transmembrane structure as ORs detecting plant volatiles. Together with an Orco co-receptor, a heteromeric complex is formed with the characteristics of a cation non-selective ion channel gated by pheromone ligands (Sato et al., 2008). Once the ligand couple to a receptor, an action potential is generated. The

axons of OSNs make up the antennal nerve, and project directly to the primary olfactory center of the brain, the AL (Reviewed by Martin et al., 2011).

Four types of sensilla are so far identified in *H. armigera*: the styloconica, chaetica, coeloconica, and trichodea (Diongue et al., 2013). Sensilla trichodea represents the majority of male sensilla and are dedicated to detection of sex pheromones. Three different types of trichoid sensilla are present: type A, B, and C, with each sensillum housing two OSNs. The majority is type A, which exhibits a strong and selective response to Z11-16:Ald. Type B and C are less abundant. While type B display a strong response only to Z9-14:Ald, type C is less specific and responds to Z9:14:Ald, Z9-16:Ald and Z11-16:OH (Chang et al., 2016) (*see figure 1*).

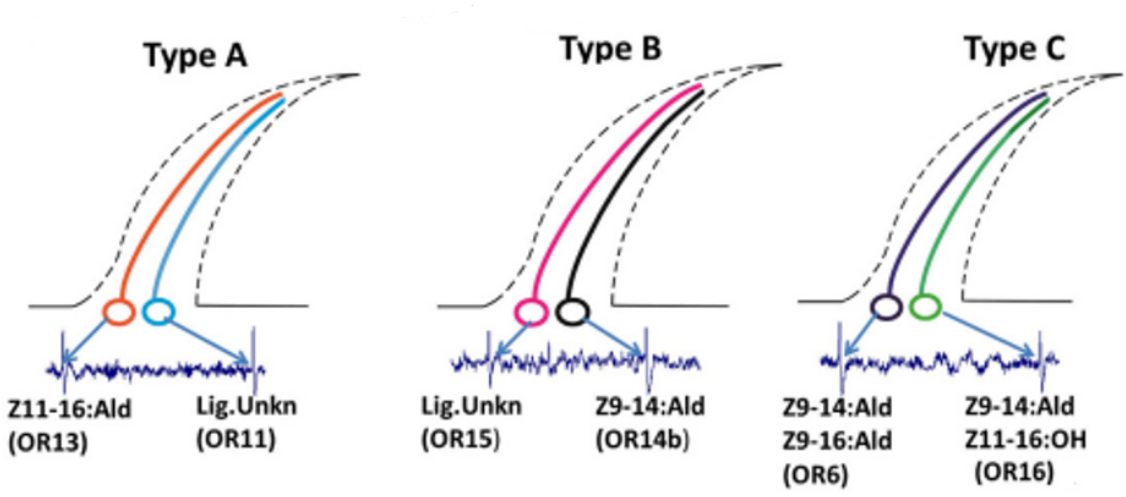

Figure 1. *Illustration of the three sensilla trichodea types in H. armigera males. Type A house OSNs expressing the OR13 receptor tuned to Z11-16:Ald, and OR11 which tuning preference is not yet known. Type B house OSNs expressing OR15 with unknown tuning preference, and OR14b tuned to Z9-14:Ald. Type C is housing OR6 tuned to Z9-14:Ald, and Z9-16:Ald, and OR16 tuned to Z9:14:Ald and Z11-16:OH. From Chang et al., 2016.*

Even though the peripheral organization of the olfactory system is generally strictly defined, individual differences in odor perception have been observed across individuals of the same species. In a study on OR polymorphisms and natural variation in olfactory behavior in the fruit fly, *Drosophila melanogaster*, Rollmann et al. (2010) reported that variations in

OR genes arising throughout evolution can contribute to individual differences in olfactory behavior, hence inducing slight changes in olfactory perception.

1.3 The Antennal Lobe

The AL is the primary olfactory center in the insect brain, analogous to the olfactory bulb in vertebrates. OSN axons enter the AL and project directly to dense, spherical neuropils, so called glomeruli. As mentioned above, the system is arranged in such a way that OSNs expressing the same type of receptor converge into the same one or two glomeruli, creating an odotopic map (Reviewed by Martin et al., 2011). In the AL, pheromones and general odorant sensory inputs are processed separately: while ordinary glomeruli receive input from OSNs tuned to plant compounds, a specialized group of enlarged glomeruli, the macroglomerular complex (MGC), encodes sex pheromone information (Reviewed by Galizia & Rössler, 2010). About 80 glomeruli have so far been identified in the *H. armigera* male, three of them making up the MGC (Zhao et al., 2016). Within the glomeruli, OSNs form synaptic connections with two main categories of second-order neurons: local interneurons (LNs) and projection neurons (PNs). The LNs are restricted to the AL where they interconnect the glomeruli by arborizing in multiple glomeruli. Many of these LNs are GABAergic inhibitory neurons playing a significant role in shaping the odor information before it is conveyed to higher-order brain areas (Christensen et al., 1993; Berg et al., 2009).

The PNs, on the other hand, convey sensory information to higher-order brain areas, mainly to the calyces of the mushroom bodies and the lateral horn (LH). PNs are either uniglomerular, meaning that they only innervate one glomerulus, or multiglomerular, extracting combined olfactory information from numerous glomeruli (Reviewed by Galizia & Rössler, 2010). This anatomical arrangement underlies the complex firing patterns of the AL glomeruli in response to different odors (Reviewed by Christensen & Hildebrand, 2002). The PNs have their cell bodies located in one of three distinct cell clusters surrounding the AL glomeruli – the lateral, medial, or anterior cell cluster. The largest cluster, the lateral, contains all the LN as well. The medial and anterior clusters, therefore, consist of PN cell bodies exclusively (Homberg et al., 1988).

A third category of AL neurons are the centrifugal neurons (CNs), which make up a small group thought to play a modulatory role. Their axons project into AL glomeruli and provide feedback information from various other brain regions (Anton & Homberg, 1999,

p.117). Different types of CNs have been identified, among them serotonergic (Dacks et al., 2006) and octopaminergic (Dacks et al., 2005).

1.3.1 The Macroglomerular Complex. The MGC is located dorsally in the AL, at the entrance of the antennal nerve (Christensen & Hildebrand, 1987). In *H. armigera*, it consists of three glomeruli, the enlarged cumulus, and two smaller units, the dorsomedial posterior (DMP) and dorsomedial anterior (DMA) (Zhao et al., 2016) (*see figure 2*).

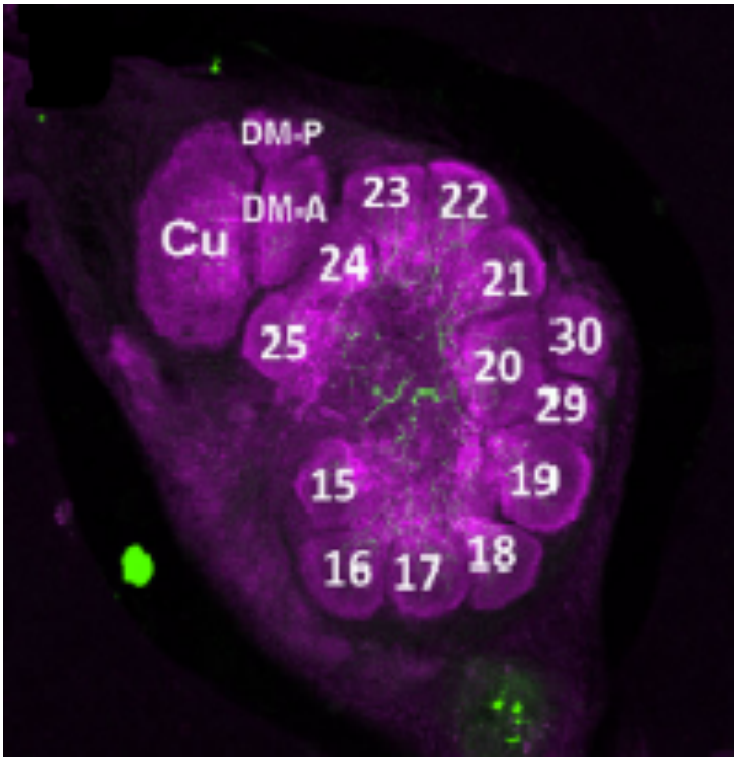

Figure 2. *Frontal view of the right H. armigera male antennal lobe. The subcompartments of the MGC are marked as Cu (cumulus), DM-P (dorsomedial posterior) and DM-A (dorsomedial anterior). Ordinary glomeruli are marked as numbers. From Zhao et al., 2016.*

Based on current understandings, the cumulus and DMP are dedicated to processing input about sex pheromones, and the DMA to processing input about the behavioral antagonists (Wu et al., 2015). Cumulus is thought to be exclusively activated by the primary pheromone component of *H. armigera*, Z11-16:Ald. The DMP is mainly activated by Z9-16:Ald, the secondary pheromone component, and the DMA by the interspecific component Z9-14:Ald (Berg et al., 2014). Interestingly, the DMP is more sensitive to Z9-14:Ald than the DMA when presented in low concentrations, but the DMA shows responses with similar

intensity when exposed to higher concentrations. When activated, the DMA responses elicit an antagonistic behavior in a male moth (Wu et al., 2015). The MGC allows for high sensitivity even though the male-specific OSNs converge with a smaller amount of PNs in comparison with the plant-odor OSNs targeting the ordinary glomeruli (Reviewed by Deisig et al., 2014).

1.4 Antennal Lobe Tracts

In the moth, information from the AL to the higher centers of the brain is conveyed by PNs through six distinct tracts (Homberg et al., 1988). Among the most studied are the medial ALT (mALT), the mediolateral tract (mlALT), the lateral ALT (lALT), and the transverse ALT (tALT) (Ian et al., 2016[a]) (*see figure 3*).

1.4.1 mALT. The mALT is the most prominent tract, including almost half of all PNs in a male moth (Homberg et al., 1988). Even though there are several sub-types of medial-tract PNs, the most frequently encountered are the uniglomerular neurons with dense arborizations filling only one glomerulus (Homberg et al., 1988; Ian et al., 2016[b]). These PNs innervate the calyces of the mushroom bodies (MB) before extending their terminal axons in the lateral protocerebrum, including the lateral horn (LH). Their cell bodies are either linked to the medial cluster or the lateral cluster. Morphologically, these neurons are very alike and display similar projection patterns. The uniglomerular medial-tract neurons constitute the main pathway between the AL and the mushroom body calyces (Ian et al., 2016[a]). These PNs play an important role in establishing odor memory. In addition to the PNs in the mALT, a small portion of the neurons in this tract are CNs, providing feedback from higher order brain regions to the AL.

1.4.2 mlALT. The mlALT is a relatively thin tract projecting directly to the LH without innervating the calyces. PNs in this tract are multiglomerular with a considerable amount of them being GABAergic (Berg et al., 2009). Since neurons making up the mALT and mlALT terminate in several overlapping areas (except for the calyces), it is suggested that they are part of a neural circuit involved in transferring unified information to third-order regions (Ian et al., 2016[b]).

1.4.3 lALT. The lALT consists of a heterogenous group of neurons that are both uni- and multiglomerular. At the exit of the AL they form a shared bundle but later proceed along

different routes (Ian et al., 2016[a]). The lateral-tract PNs exit the AL more ventrally than the above-mentioned sub-types and project laterally towards the lateral protocerebrum, with only a few neurons innervating the calyces (Ian et al., 2016[b]). Some lateral-tract neurons project to the contralateral protocerebrum as well (Homberg et al., 1988). Since the lALT PNs terminate in several areas distinct from neurons in the mALT and mlALT, they are assumed to take part in distinct neural circuits (Ian et al., 2016[b]).

1.4.4 tALT. The tALT is a relatively newly identified tract which, in similarity to the mlALT, joins the mALT before curving laterally, then targeting the calyces of the mushroom bodies and the LH. However, the tALT is passing laterally posteriorly of the mlALT (Ian et al., 2016[a]).

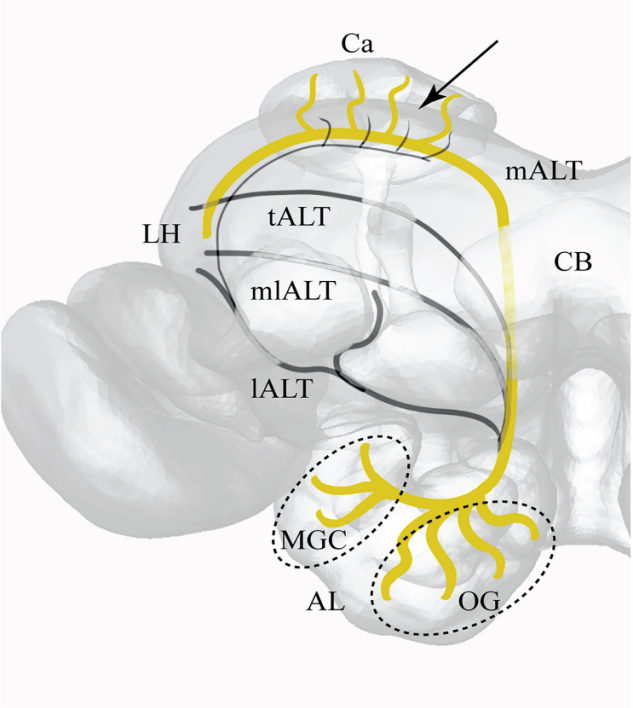

Figure 3. *Illustration of the right hemisphere showing AL tracts and major brain areas. mALT (medial Antennal Lobe Tract), mlALT (mediolateral Antennal Lobe Tract), lALT (lateral Antennal Lobe Tract), tALT (transverse Antennal Lobe Tract), AL (Antennal Lobe), MGC (Macro Glomerular Complex), OG (Ordinary Glomeruli), CB (Central Body), Ca (Calyx), LH (Lateral Horn). From Ian et al., 2017.*

1.5 Higher Order Brain Areas

As mentioned above, the main areas of the brain to which the PNs send information from the AL are the calyces and the LH (Ian et al., 2016[b]). In the calyces, PNs (mainly medial-tract neurons) synapse with tiny intrinsic interneurons called Kenyon cells (Laurent & Naraghi, 1994). The MB functions as a central processing unit, with the calyces being the input areas and the lobes serving as output. It is a heterologous structure, containing several subsystems involved in important functions, such as feedback connectivity, learning, and memory (Reviewed by Stopfer, 2014). While the MB Kenyon cells only combine input from a small assortment of glomeruli, each PN establishes contacts with numerous Kenyon cells. However, Murphy et al. (2008) conducted a study showing that the tuning of Kenyon cells differed from individual to individual, showing little stereotypy. It appears to be individual differences in the glomerular input patterns, which is actually consistent with the assumption that the MB is concerned with learned behaviors (Fişek & Wilson, 2014). Interestingly, PNs tuned to pheromones and plant odorants target distinct regions both in the calyces and in the LH (Zhao et al., 2014), indicating a spatial segregation of information related to the two odor categories at the higher levels as well.

The LH is mainly processing olfactory information and is assumed to be mediating odorant responses that are not due to learned associations or memory (Reviewed by Fişek & Wilson, 2014). PNs´ connectivity in the LH indicates a stereotypical, more hardwired pattern in contrast to the seemingly more individually and flexible connectivity in the MB (Reviewed by Schultzhaus et al., 2017). Interestingly, it has been reported that male-specific medial-tract PNs in the *H. assulta* seem to be spatially organized in the lateral protocerebrum so that conspecific and interspecific signal information target partially different areas (Berg et al., 2014; Zhao et al., 2014).

1.6 Calcium Imaging

Over the last few decades, calcium imaging has emerged as a great tool for optical imaging of neuronal activity. It allows for recording of multiple structures simultaneously, making it a beneficial method for *in vivo* observations.

Calcium acts as an intracellular second messenger, controlling a variety of cellular processes. Influx of calcium ions plays a substantial role, for example, in induction of action

potentials (Grienberger & Konnerth, 2012). At resting levels, the intracellular concentration of calcium is approximately 100nM. However, during activation, the concentration can reach up to 1000nM, making intracellular calcium concentration a great indicator of neuron activity (Reviewed by Berridge et al., 2000). To be able to perform calcium imaging from neural tissue, fluorescent dye binding to calcium ions has to be applied to the preparation. Several distinct dyes are used for this purpose (Tsien, 1989). In this project, the fura-2 dextran was administered into the calyces of the MB. The dye will then be carried, via retrograde transportation by the medial-tract PNs to the AL glomeruli. Calcium imaging is advantageous in that it can provide with data from a big population of neurons in comparison to single cell recordings where registrations of activity is performed only for one individual neuron. As an *in vivo* method, calcium imaging makes it possible to observe natural brain activity as it occurs, making it favorable over *in vitro* methods (Helmchen & Waters, 2002).

1.7 Dose Response

Traditionally in calcium imaging experiments, high concentrations of odors have been used for stimulation to achieve a good signal to noise ratio. However, concentrations that are too high may fail to mimic naturally occurring olfactory signals and therefore contribute to irrelevant results. By performing systematic measurements with different stimulus concentrations, it is possible to plot dose response curves, which may point to the optimal concentration for stimulation. The lowest detectable concentration and the highest concentration before reaching saturation can also be of interest.

A dose response relationship is defined as: "*A relationship between exposure/dose and response/effect that can be established by measuring the response relative to an increasing dose*" (Moffett et al., 2007, p. 101). The pattern is often in line with a sigmoidal curve (*see figure 4*), which pictures a steep increase in response until reaching a plateau. Once reaching the plateau, no increase in concentration will have an additional effect, the highest possible response has been reached. Previously, dose response curves of individual OSNs have been reported in heliothine moths, based on electrophysiological experiments (Berg et al., 1995; Berg & Mustaparta, 1995). In the current project, I will utilize calcium imaging measurements of odor-evoked responses from the MGC units in the *H. armigera* to establish the dose response relationship for male-specific medial-tract PNs.

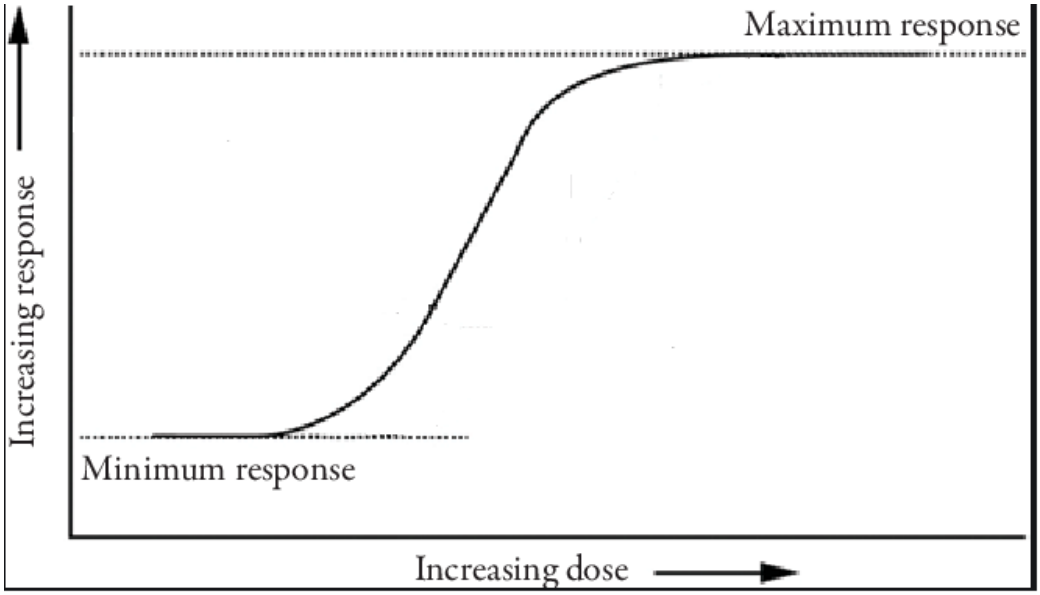

Figure 4. *Illustration of a dose response relationship. The response is increasing with an increasing dose until reaching the maximum response, or saturation point. Modified from Gough et al., 2011.*

1.8 Aims

The aim of the present project was to explore sensitivity of the mALT PNs confined to three MGC glomeruli: the cumulus, the DMP and the DMA. Optical imaging of calcium fluctuations were registered in response to different concentrations of the primary pheromone, Z11-16:Ald, secondary pheromone, Z9-16:Ald, and interspecific component, Z9-14:Ald. To obtain relevant data material, the following experimental and computational stages of the project had to be performed:

1. Successful retrograde staining of the mALT PNs.
2. Collection of a satisfactory amount of data suitable for analysis.
3. Mapping out glomeruli by processing the data in KNIME.
4. Visualization of average traces and response curves by the using the software programs R and Python.

The principal aim of the project presented here, was to define the dose response relationship for odor-evoked activation of medial-tract MGC neurons.

Sub-goals:

- To define the lowest concentration eliciting a detectable signal.
- To define the highest concentration before reaching saturation.
- To explore whether the three relevant stimuli, two pheromone constituents and one interspecific signal, activate the MGC PNs in a similar manner.

2. Materials and methods

2.1 Insects

The insects used in this project were male moths of the species *Helicoverpa armigera* (Lepidoptera: Noctuidae; Heliothinae). For the experimental work we used 3-5 days old virgin males. The pupae were provided by Henan Jiyuan Baiyun industry Co, Ltd. in China. Both hatched and unhatched moths were kept in a climate chamber with 60% humidity and a day-night cycle of 14-10 hours. The moths were placed in cylindrical or squared boxes with access to 10% sucrose solution. A maximum of 5-8 moths were placed in each box.

There are no ethical guidelines in Norway concerning the use of moths in research. However, the insects were treated ethically, avoiding any unnecessary harm or distress.

2.2 Preparation

First, the insect was taken out of the climate chamber, put in a small plastic container in the refrigerator at 4 °C for about 10-20 minutes for sedation. Next, the insect was placed in a small plastic tube, with only the head and antennae accessible. The head was fixed with dental wax (Kerr Corporation, Romulus, MI) for stabilization. All the further preparations were executed under a Leica DMC 4500 microscope. First, all scales were removed by scraping them off with forceps. Then, the dorso-posterior part of the head capsule was cut open with a razor blade knife and removed, making it possible to access the calyces. Trachea and muscles covering the brain were removed. Fine forceps was used to pluck a little hole in the brain anteriorly to the calyces to enable easier access with electrodes. Glass electrodes loaded with the dye Fura-2 dextran (10,000 MW, in 2% BSA; Molecular Probes) were then used to penetrate the brain and stain PNs of the mALT from the calyces. Depending on the

amount of dye on each electrode, between two and four electrodes were used for staining each individual insect. The glass electrodes were made using a micropipette puller from SUTTER INSTRUMENT CO. MODEL P-97. The dye, Fura-2 dextran, was kept in a freezer and only taken out just before the dye application, which was executed manually under the microscope. To limit light exposure, the whole preparation was executed in a darkened room.

Ringer solution (in mM: 150 NaCl, 3 CaC12, 3 KC1, 25 Sucrose and 10 N-tris (hydroxymethyl)-methyl-2-amino-ethanesulfonic acid, pH 6.9) was used to keep the brain moist during preparation and was also used to rinse the brain 3-4 times to remove any excess dye. After dye application, the exposed part of the brain was covered with a fine sheet of paper soaked in ringer solution to prevent desiccation. The insect was kept in a dark humid box in the refrigerator overnight, allowing the dye to travel retrogradely from the calyces to the AL via the mALT.

The next day, the fine sheet of paper was removed, and the dorsal part of the head capsule was cut open to provide a view of the AL. Excess trachea and muscles that could disturb the imaging were cleared away. To immobilize the antennae during the experiment, Eicosane (C20H42) was applied (Sigma-Aldrich). Due to the low melting point, no harm was caused.

2.3 Odor Stimulation

As odor stimuli, three different components including two pheromones and one interspecific component, were used in this study: the primary pheromone *cis*-11-hexadecenal (Z11-16:Ald, coded as A), the secondary pheromone cis-9-hexadecenal (Z9-16:Ald, coded as B), and the interspecific component *cis*-9-tetradecenal (Z9-14:Ald, coded as C) (*see table 1*). Six different concentrations of each pheromone were made, ranging from concentration 10^{-3} to 10^{-8}. 20 µl of a solution was applied on a filter paper inserted into a 150 mm glass Pasteur pipette. Each microliter of a solution gives 0.5 µg of a component. Thus, applied 20 µl corresponds to 10 µg of a stimulus for concentration 10^{-3}, 1 µg - for concentration 10^{-4}, and so on. The components were diluted in mineral oil (Across Organics). When running the experiments codes like A8 and B7 were used. A8 represented the concentration $A10^{-8}$ and B7 $B10^{-7}$, and so forth. Each stimulus had two trials and was separated by using _1 and _2 (for example A8_1). For processing in RStudio (*see 2.5 Data Processing and Statistical Analysis*)

the codes had to be changed to letters only, ranging from for example Aa-Af, where Aa represents $A10^{-3}$ and Af $A10^{-8}$, and so forth.

		Code
Primary pheromone component	Z11-16:Ald	**A**
Secondary pheromone component	Z9-16:Ald	**B**
Interspecific component	Z9-14:Ald	**C**

Table 1. *Overview of stimulations used in the experiment.*

To make stimuli, small pieces of paper were folded and inserted into glass tubes using sterilized forceps. Five microliters of each stimulus compound were carefully applied on the filter paper avoiding contamination of the outer part of the tube. When not in use, the stimuli tubes were stored in a freezer with parafilm covering both ends, preventing the stimuli from weakening.

2.4 Imaging

First, the moth was placed under an epifluorescent microscope (Olympus BX51WI), allowing for imaging of the dorsal part of the AL. The microscope was set up with a 20x/1.00 water immersion objective (X1UMPlanFL N). Ringer solution was applied to enclose the space between the objective and the preparation. Image recordings were acquired by a CMOS camera (Hamamatsu ORCA-Flash 4.0 V2 C11440-22CU). A polychromator (TILL Photonics

Polychomatro V) was used to excite the preparation with 340nm and 380nm wavelength light at consistent intervals. A dichroic mirror together with an emission filter (490-530) was used to assure separation of excitation light (340/380nm) and emission light (505/520nm peak). Recordings were acquired using the program Live Acquisition V2.6.0.35 (TILL Photonics). The image binning size was set to 4x4, with each recording lasting 10 seconds with 100 frames, resulting in 100 milliseconds in each frame. The odor stimulation started 3 seconds after onset of each recording. Every stimulus was bestowed twice, with 1 minute between each stimulation. FEI Offline Analysis V2.6.0.35 was used for the preliminary signal evaluation.

2.5 Data Processing and Statistical Analysis

KNIME Analytics Platform 2.12.2 and the ImageBee plugin (Strauch et al., 2013) were applied for processing of the raw data. The program consists of "nodes" and use a workflow methodology in which each node must be completed before the data is further processed by the next node. The workflow used is separated into an upper and lower path (*see figure 5*).

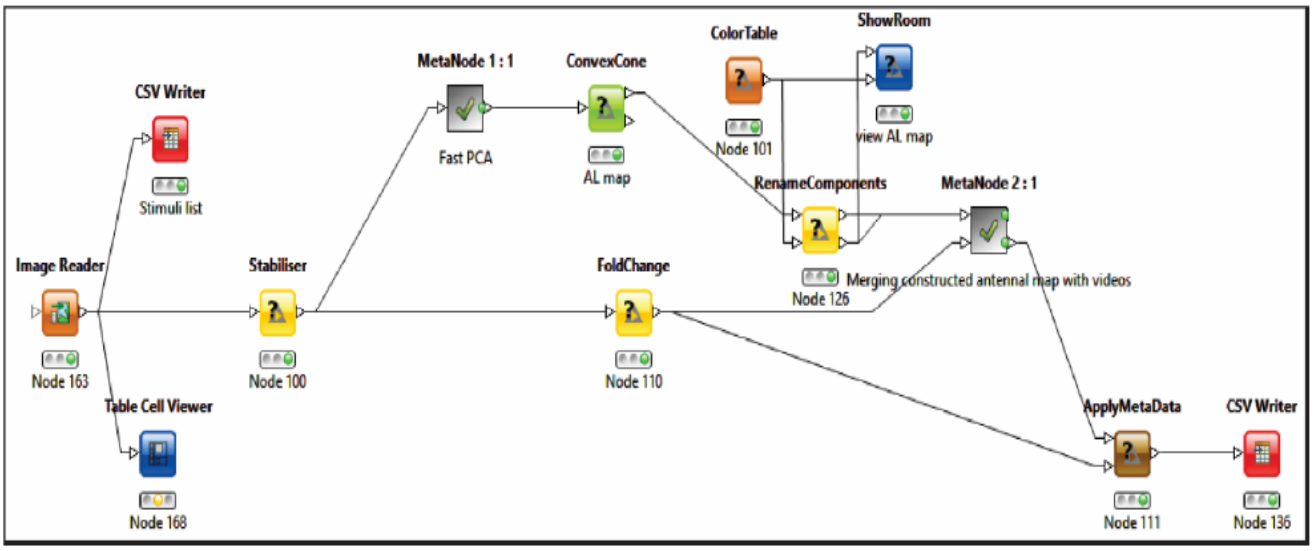

Figure 5. *The KNIME workflow which provided two outcomes, one file for stimuli list and one for time traces for fluorescent values respectively.*

First, the unprocessed movies are read by the “Image Reader”, and the “CSV Writer” node provide a .csv file containing a list of all stimuli. Next, the raw data is run through a “stabilizer” which provides a movement correction. The upper path creates an estimated AL map with identifiable glomeruli by conducting a z-score normalization, meaning subtracting the mean and dividing by standard deviation. A principal component analysis (PCA) algorithm will further identifies correlations between neighboring pixels, and a convex cone algorithm recognizes areas with the highest correlations. The AL map can be viewed and downloaded in the “ShowRoom” node. In the lower path, normalization is conducted for each pixel using its mean value during the interval before stimulus application, resulting in a baseline set to zero. The responses seen are relative to baseline. In the end, the constructed AL map is combined with the videos holding the baseline data, creating a time-series for all glomeruli that generates a .csv format output.

The program RStudio (1.1.463) was used for creation of glomerular mean traces for each preparation. An output file was created based on the combination of the stimulus list and the time-series. Python (3.7.4) was used to create dose response curves for every MGC glomerulus in each preparation.

3. Results

A total of 12 insects underwent the full experimental procedure with successful staining and imaging. Raw data from these preparations were processed in KNIME in order to determine whether all three glomeruli were clearly visible in the AL map generated by the software (*see figure 6*). Among the 12 KNIME datasets, 3 met the criterium of displaying recognizable MGC units. These 3 datasets are presented here in the results.

With the aim to identify the most suitable concentration for calcium imaging, mean traces obtained from analysis in KNIME and RStudio are presented in the subsequent section together with dose response curves made in Python. In addition, a comparison between raw data traces and mean traces was conducted, and the most prominent discrepancies are presented here in the results as well. The traces represent odor-evoked responses to the different concentrations of pheromone and interspecific components in the subareas of the

MGC. The results will be presented preparation by preparation, in the order: Cumulus, DMP, and DMA.

3.1 Preparation 1

The data collected from preparation 1 provided the best results with a strong coherence between raw data and processed data for all three MGC glomeruli.

3.1.1 Cumulus Responses.

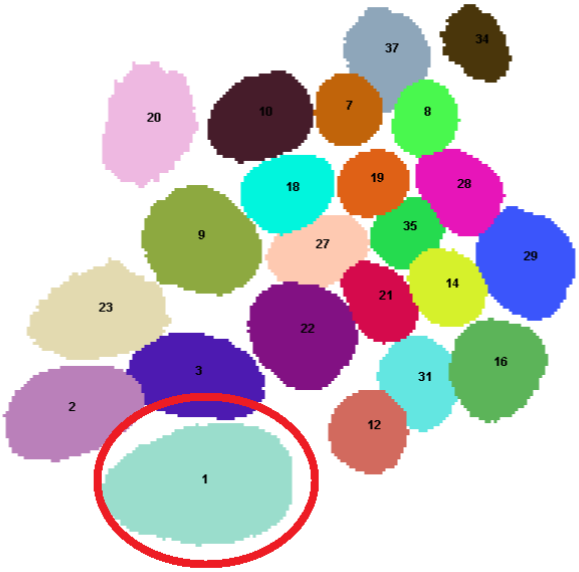

Figure 6. *Antennal lobe map generated by KNIME. The cumulus (1) is outlined.*

Cumulus (*Figure 6*) demonstrated a strong response to the primary pheromone component, A, when stimulated with concentrations 10^{-3} and 10^{-4}, whereas lower concentrations elicited weak or no responses. For stimulation with the secondary pheromone component, B, no cumulus activation was observed at any concentration. During exposure of the interspecific component, C, cumulus displayed strong responses to the concentrations 10^{-3} and 10^{-4}, and no activation when stimulated with the lower ones. While figure 7a displays mean traces of responses to all three stimuli, A, B, and C, figure 7b shows the dose response relationship for the same stimuli.

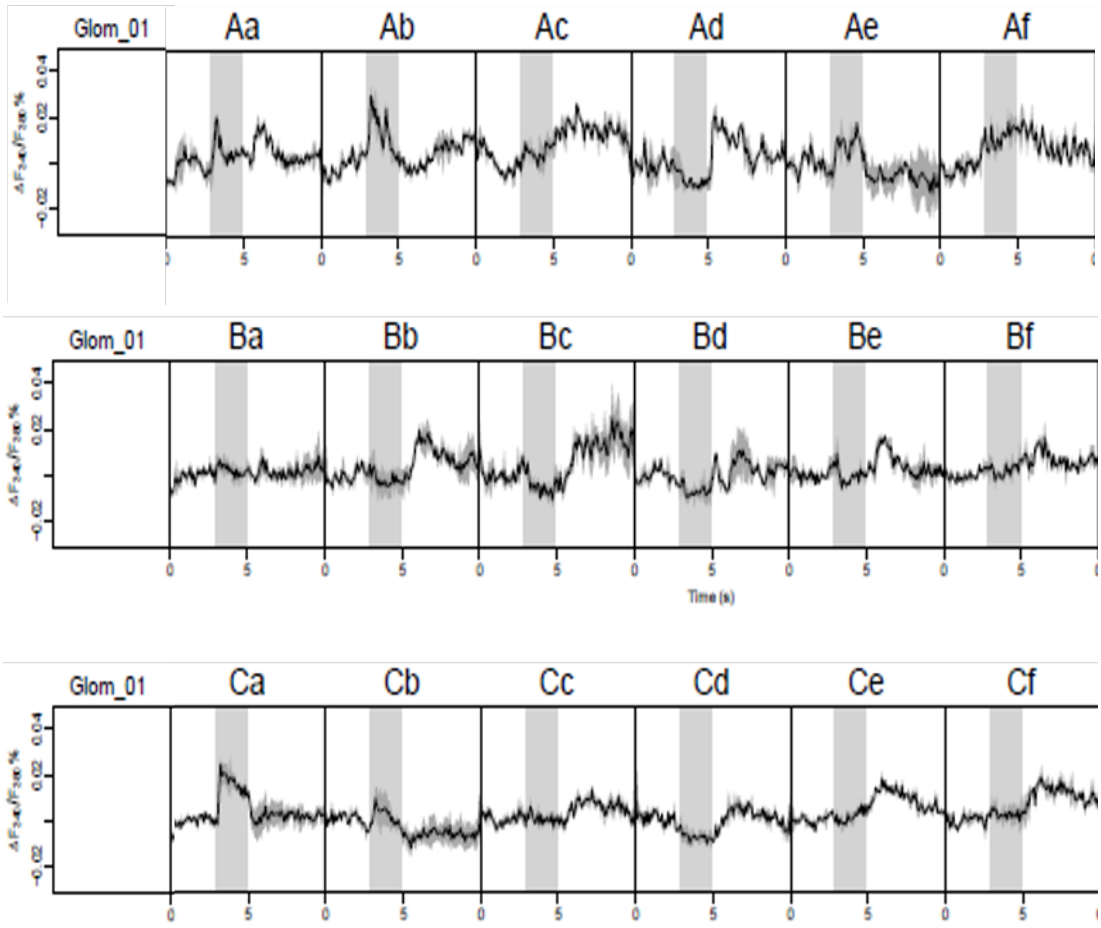

Figure 7a. *Mean traces of cumulus responses in preparation 1 to the primary (upper), secondary (mid), and interspecific (bottom) components. The stimulus period is indicated by the gray column.*

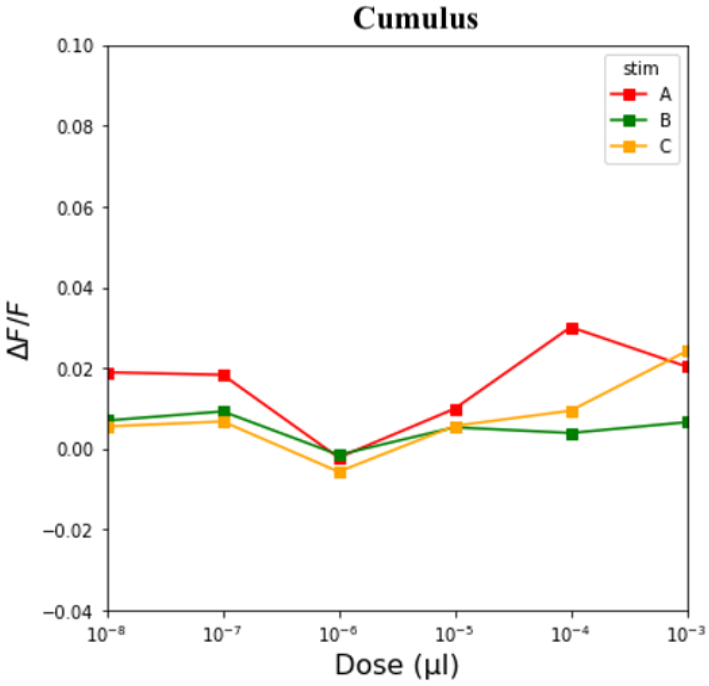

Figure 7b. *Dose response curves demonstrating cumulus responses in preparation 1. The red line named "A" indicates responses to the primary pheromone component, the green line named "B" demonstrates secondary pheromone component responses, and the yellow line named "C" indicates responses to the interspecific component.*

3.1.2 DMP Responses.

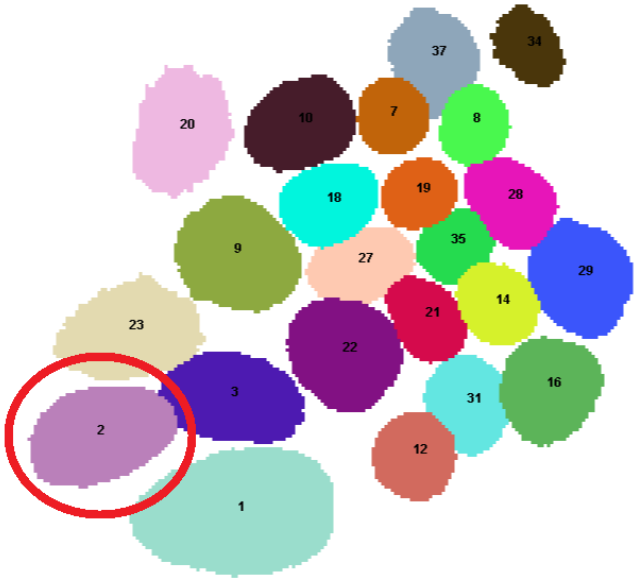

Figure 8. *Antennal lobe map generated by KNIME. The DMP (2) is outlined.*

The DMP (*Figure 8*) was activated by all three stimuli. High concentrations (10^{-3} and 10^{-4}) of the secondary pheromone component, B elicited strong responses, while the lower concentrations demonstrated no activation. The DMP was the only MGC-unit responding to this component. Concentrations 10^{-3}-10^{-5} of the interspecific component, C, elicited strong responses in the DMP as well, but no activation was demonstrated by the lower ones. Activation was also demonstrated by high concentrations (10^{-3} and 10^{-4}) of the primary pheromone component, A. Besides this, no other concentrations elicited notable responses. Here, the responses in terms of mean traces for all three stimuli are shown in figure 9a. The dose response relationship is pictured in figure 9b.

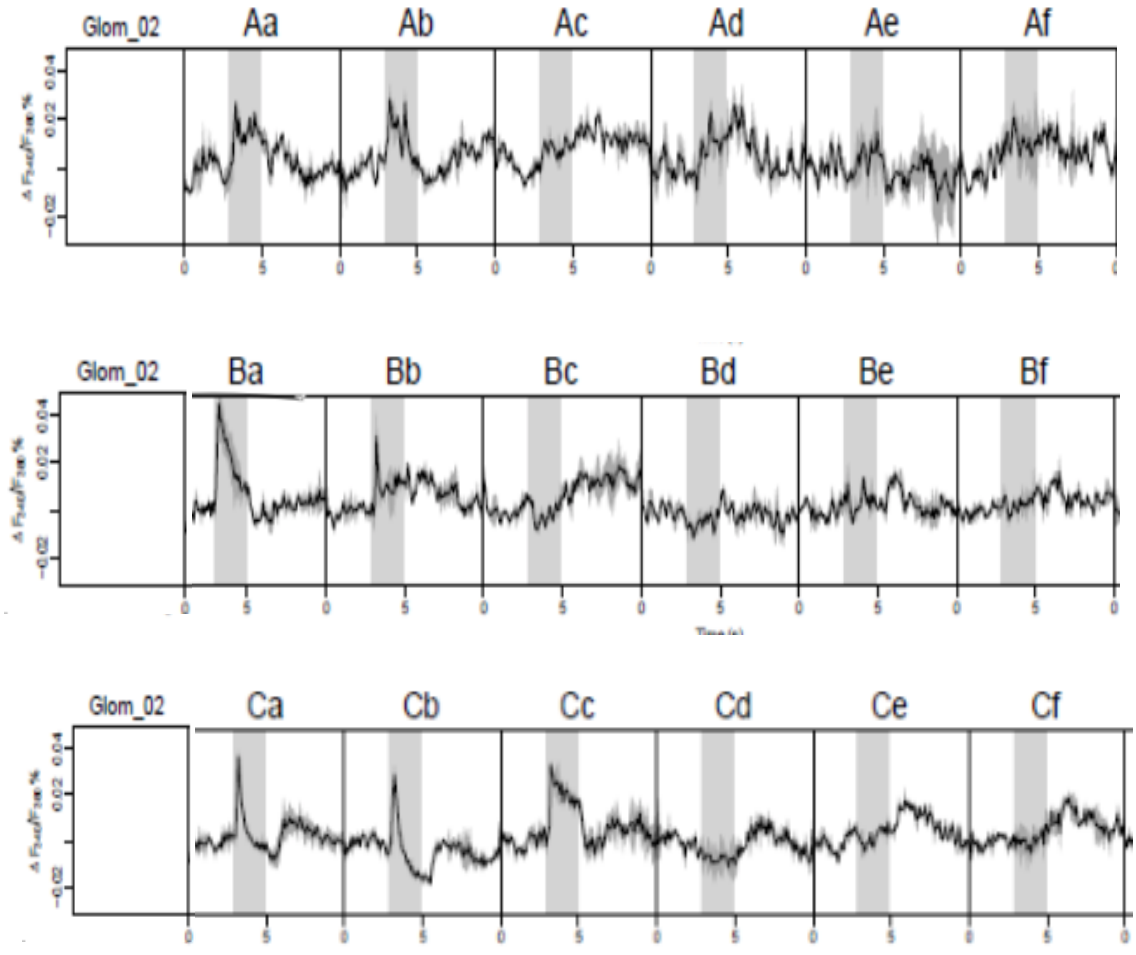

Figure 9a. *Mean traces of DMP responses in preparation 1 to the primary (upper), secondary (mid), and interspecific (bottom) components. The stimulus period is indicated by the gray column.*

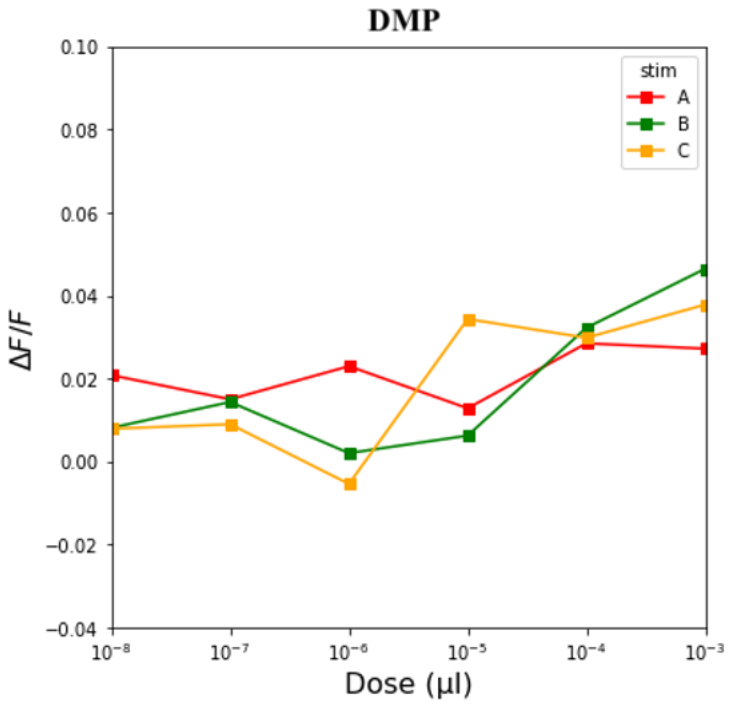

Figure 9b. *Dose response curves demonstrating DMP responses in preparation 1. The red line named "A" indicates responses to the primary pheromone component, the green line named "B" demonstrates secondary pheromone component responses, and the yellow line named "C" indicates responses to the interspecific component.*

3.1.3 DMA Responses.

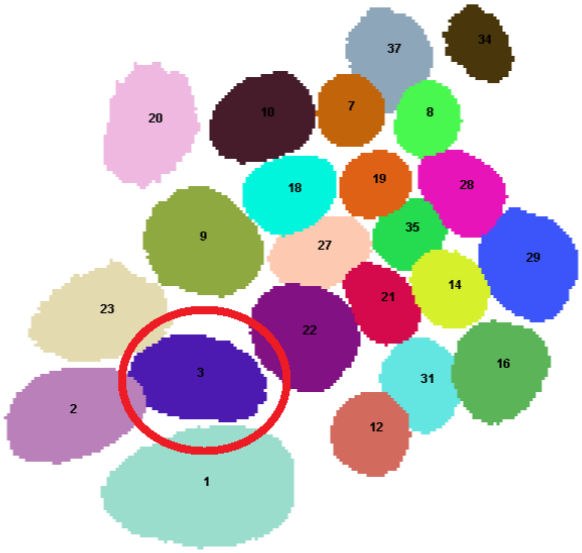

Figure 10. *Antennal lobe map generated by KNIME. The DMA (3) is outlined.*

As predicted, strong activation of the DMA (*Figure 10*) was observed when stimulated with high concentrations (10^{-3} and 10^{-4}) of the interspecific component, C. The lower concentrations did not elicit any responses. The DMA also demonstrated a strong response to the higher concentrations (10^{-3}-10^{-4}) of the primary pheromone component, A. The remaining concentrations elicited no responses. The DMA demonstrated no responses to the secondary pheromone component, B, regardless of concentration. Mean traces of all stimuli are presented in figure 11a, while figure 11b shows the dose response relationship.

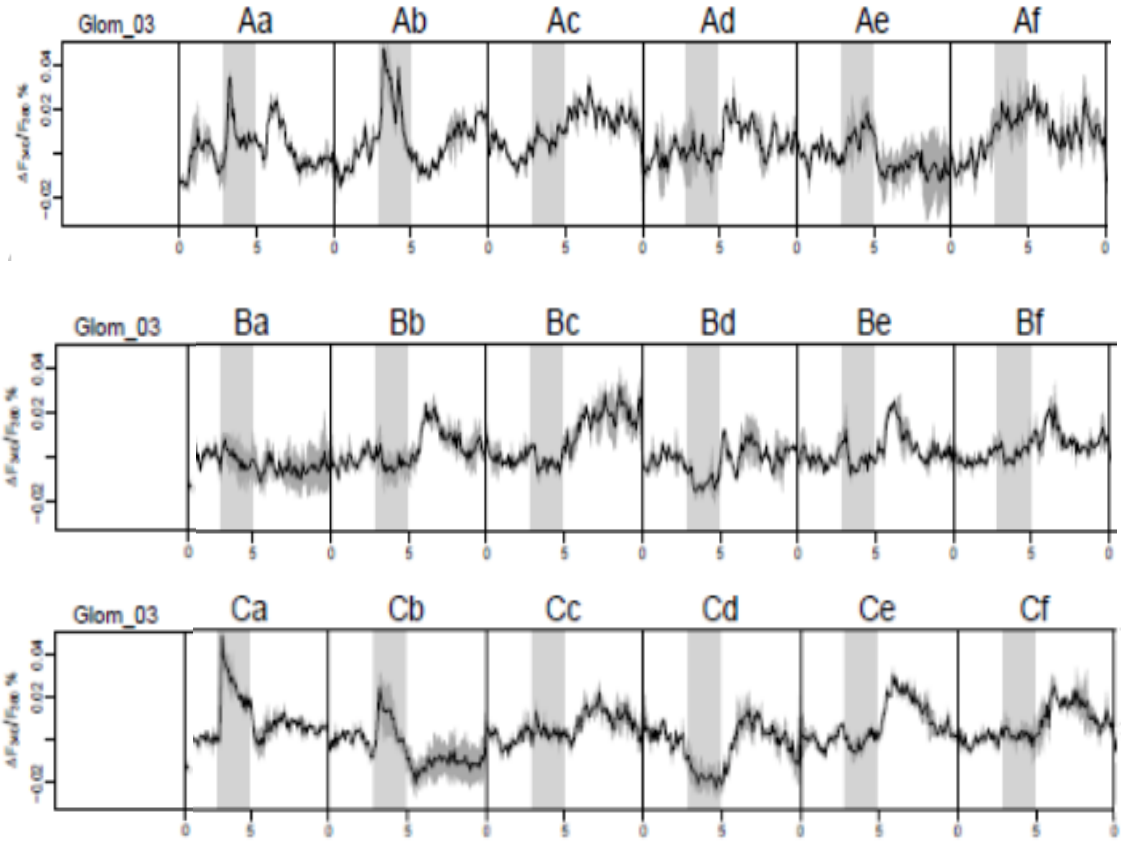

Figure 11a. *Mean traces of DMA responses in preparation 1 to the primary (upper), secondary (mid), and interspecific (bottom) components. The stimulus period is indicated by the gray column.*

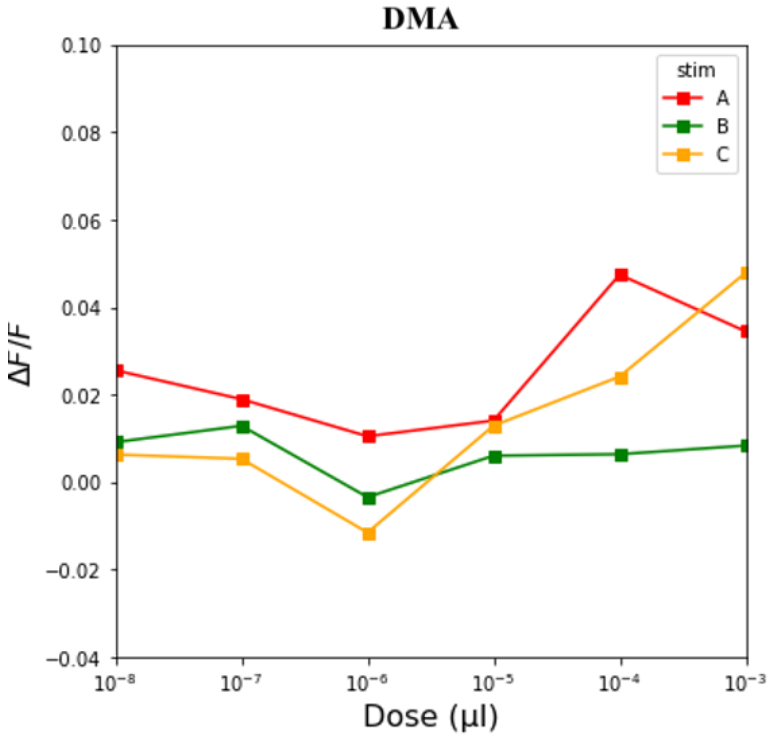

Figure 11b. *Dose response curve demonstrating DMA responses in preparation 1. The red line named "A" indicates responses to the primary pheromone component, the green line named "B" demonstrates secondary pheromone component responses, and the yellow line named "C" indicates responses to the interspecific component.*

3.2 Preparation 2

Data collected from preparation 2 provided high similarity between raw data and processed data with respect to the responses in cumulus, whereas the corresponding data for DMP and DMA showed some variation, probably due to preparation movement during the experiment.

3.2.1 Cumulus Responses. In similarity to preparation 1, the cumulus demonstrated prominent responses to high concentrations (10^{-3}-10^{-5}) of the primary pheromone component, A. Lower concentrations elicited no responses. The highest concentration of the secondary pheromone component, B, elicited a clear response, while concentrations 10^{-5} and 10^{-6} seemed to have an inhibitory effect. The interspecific component elicited no prominent responses. However, a moderate activation could be observed during stimulation with concentration 10^{-4}.

Figure 12a shows mean traces for all three stimuli, while the dose response relationship is presented in figure 12b.

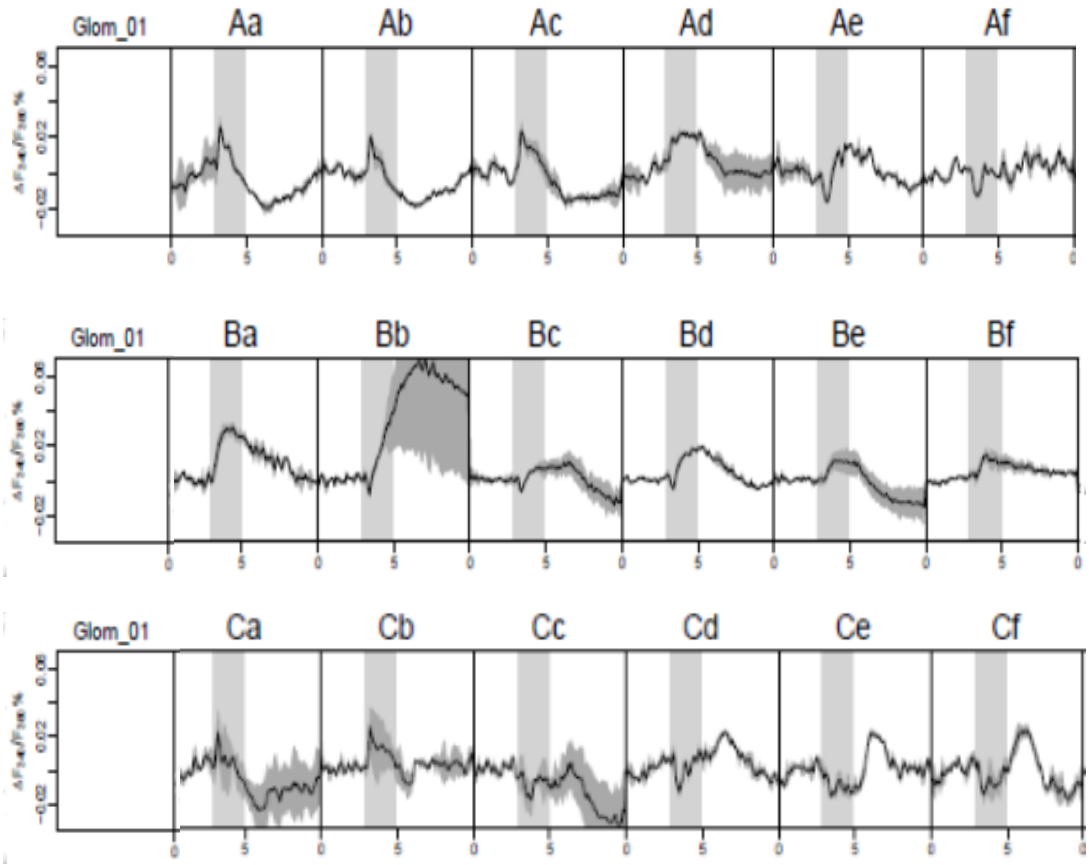

Figure 12a. *Mean traces of cumulus responses in preparation 2 to the primary (upper), secondary (mid), and interspecific (bottom) components. The stimulus period is indicated by the gray column.*

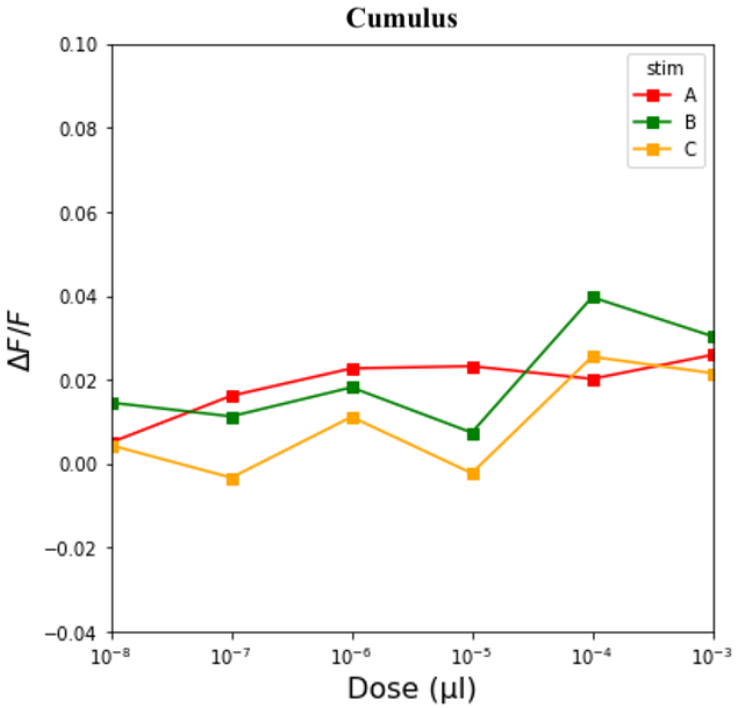

Figure 12b. *Dose response curve demonstrating cumulus responses in preparation 2. The red line named "A" indicates responses to the primary pheromone component, the green line named "B" demonstrates secondary pheromone component responses, and the yellow line named "C" indicates responses to the interspecific component.*

3.2.2 DMP Responses. Stimulation with the secondary pheromone component, B, displayed excitatory responses to concentrations 10^{-3} and 10^{-7}-10^{-8}, but also responses looking like inhibition to concentrations 10^{-5} and 10^{-6}. When stimulated with the interspecific component, C, an activation was observed during concentrations 10^{-3} and 10^{-4}. The primary pheromone component, A, elicited no responses in the DMP. Mean traces of all stimuli are presented in figure 13a. Figure 13b shows the dose response relationship.

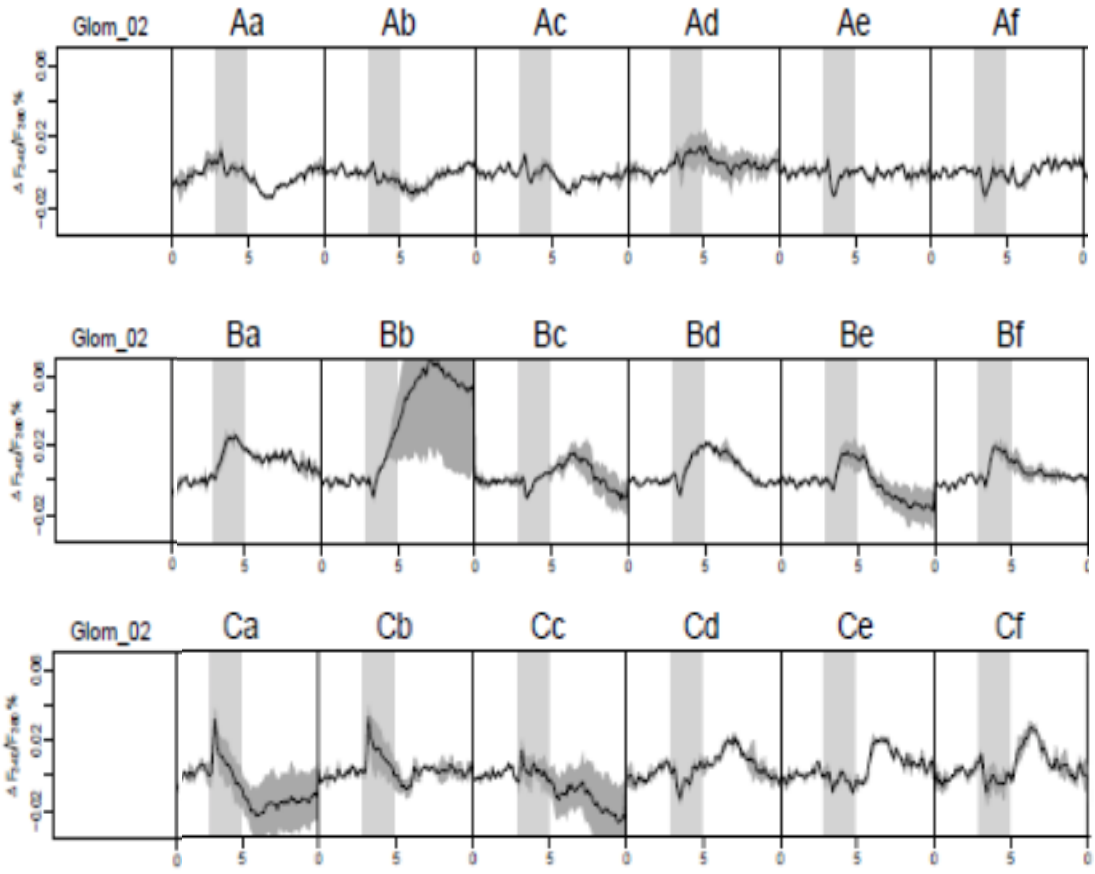

Figure 13a. *Mean traces of DMP responses in preparation 2 to the primary (upper), secondary (mid), and interspecific (bottom) components. The stimulus period is indicated by the gray column.*

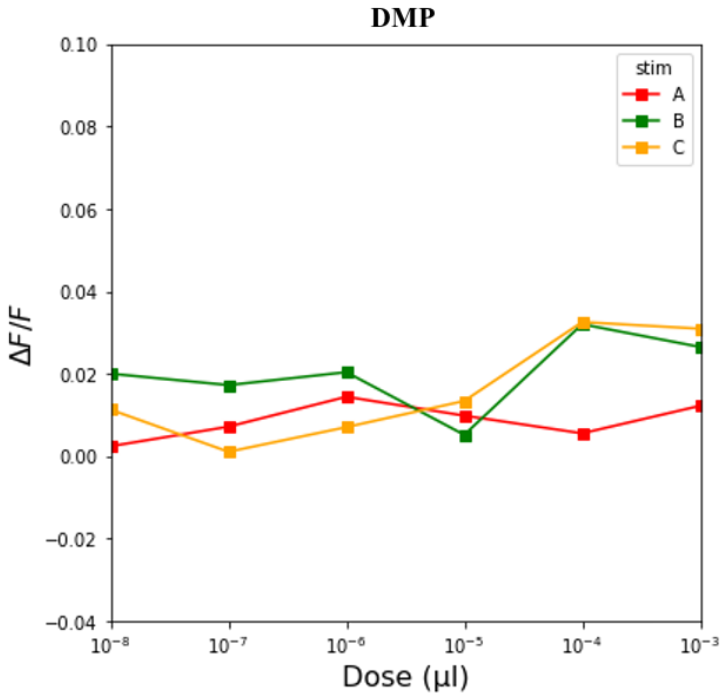

Figure 13b. *Dose response curve demonstrating DMP responses in preparation 2. The red line named "A" indicates responses to the primary pheromone component, the green line named "B" demonstrates secondary pheromone component responses, and the yellow line named "C" indicates responses to the interspecific component.*

3.2.3 DMA responses. Surprisingly enough, no prominent responses were observed during stimulation with the interspecific component, C, which is conflicting with the results from preparation 1 and previous findings (*see discussion*). During stimulation with the secondary pheromone component, B, the DMA showed various responses to all concentrations. No prominent responses occurred during stimulation with the primary pheromone component, A. However, the responses to lower concentrations (10^{-7} and 10^{-8}) can be interpreted as weak inhibition close to stimulus onset. Interestingly, when comparing the mean traces with the raw data traces for some of the concentrations, a notable discrepancy can be seen (*Figure 14c*). Figure 14a pictures mean traces of all three stimuli, while the dose response relationship is shown in figure 14b.

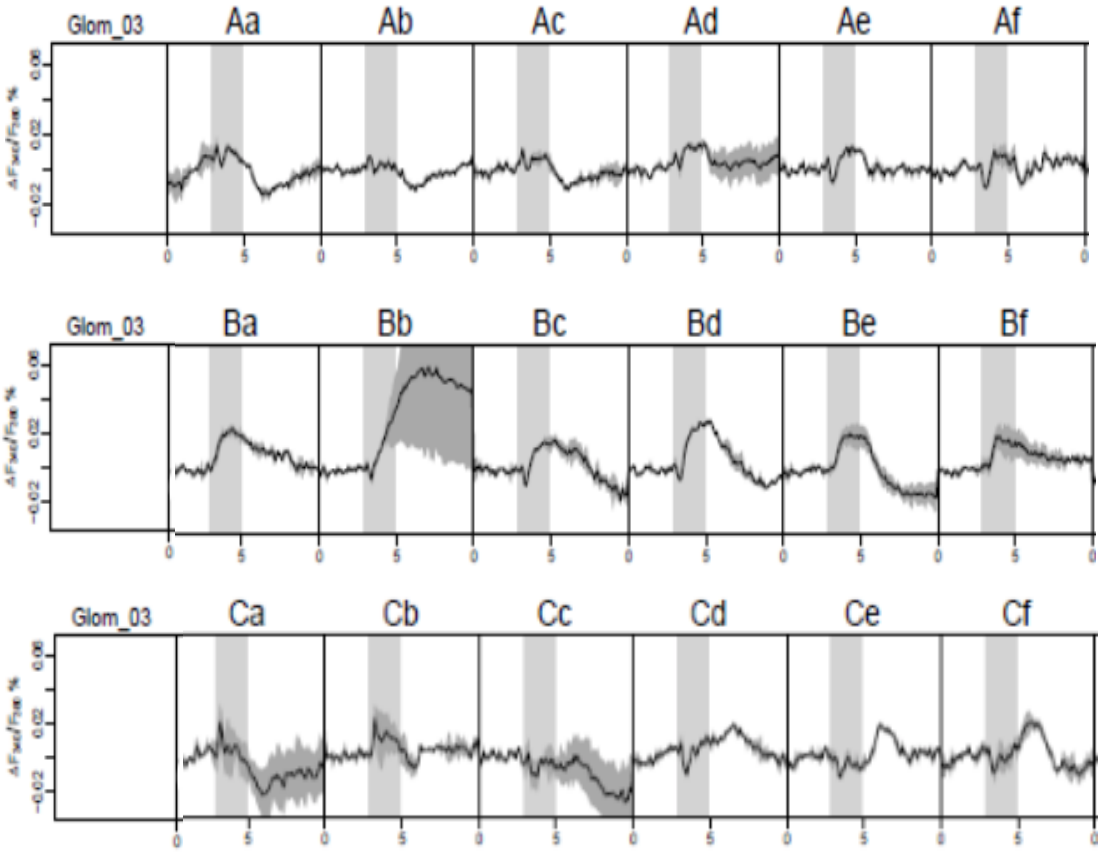

Figure 14a. *Mean traces of DMA responses in preparation 2 to the primary (upper), secondary (mid), and interspecific (bottom) components. The stimulus period is indicated by the gray column.*

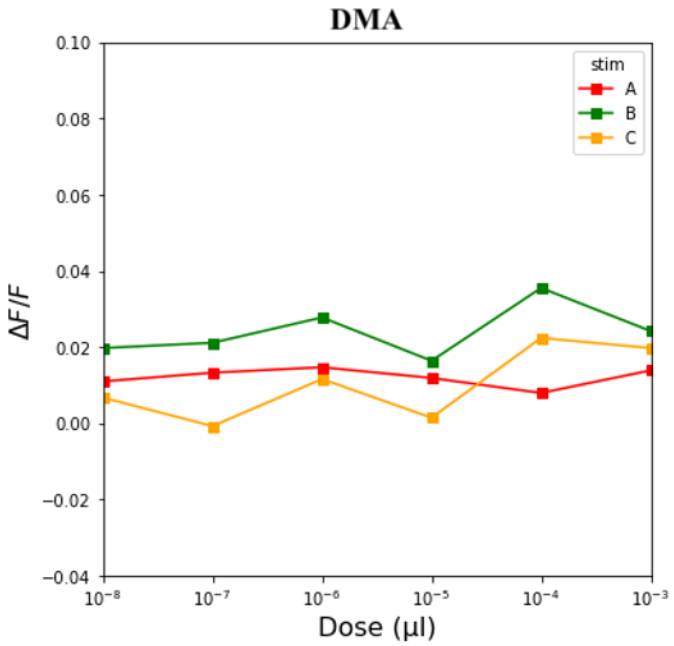

Figure 14b. *Dose response curves demonstrating DMA responses in preparation 2. The red line named "A" indicates responses to the primary pheromone component, the green line named "B" demonstrates secondary pheromone component responses, and the yellow line named "C" indicates responses to the interspecific component.*

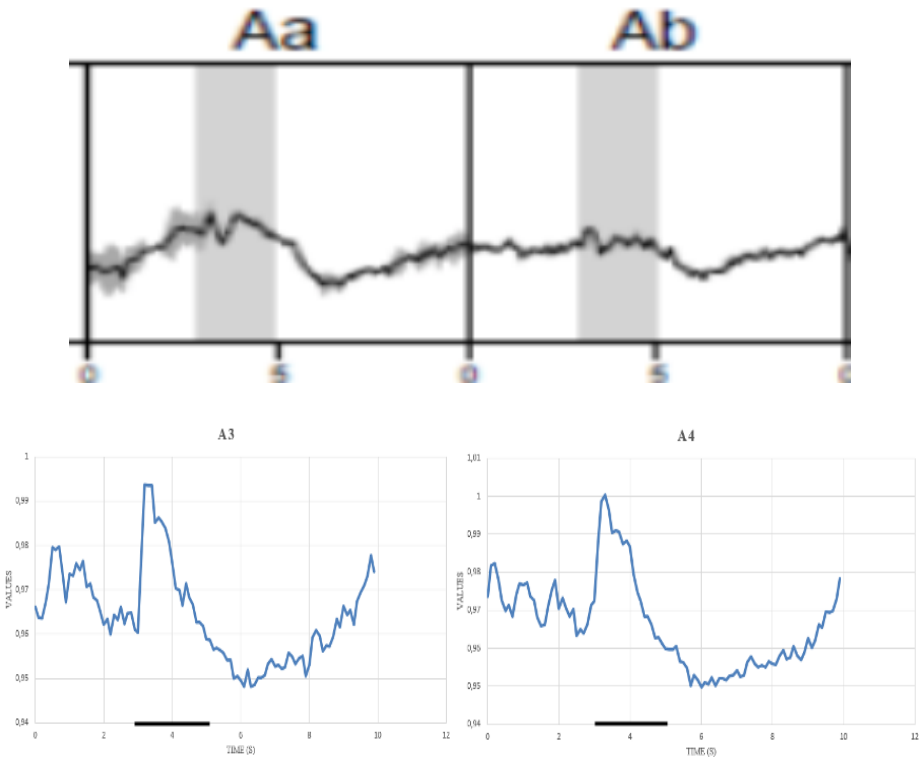

Figure 14c. *Comparison of mean traces and raw data traces in DMA in preparation 2. The black elevated lines in the raw data traces indicate the stimulation period from second 3 to 5.*

3.3 Preparation 3

Data collected from preparation 3 also provided mixed results, probably due to preparation movement. The responses in cumulus and DMP demonstrated some inconsistencies according to the raw data traces and mean traces. DMA responses, however, displayed more stability.

3.3.1 Cumulus Responses. In preparation 3, cumulus answered with the strongest responses to concentrations 10^{-5} and 10^{-6} of the primary pheromone component, A, but concentrations 10^{-3} and 10^{-4} displayed notable responses as well. The highest concentration of the secondary pheromone component, B, also demonstrated a strong response. Remaining concentrations (10^{-4}-10^{-8}) may indicate inhibition, but when comparing some of the mean traces with raw data traces, some discrepancies between the traces are visible (*Figure 15c*). Stimulation with the interspecific component, C, demonstrated responses to concentrations

10^{-4}-10^{-5} and 10^{-7}-10^{-8}. Figure 15a demonstrates mean traces for all stimuli, and figure 15b shows the dose response relationship.

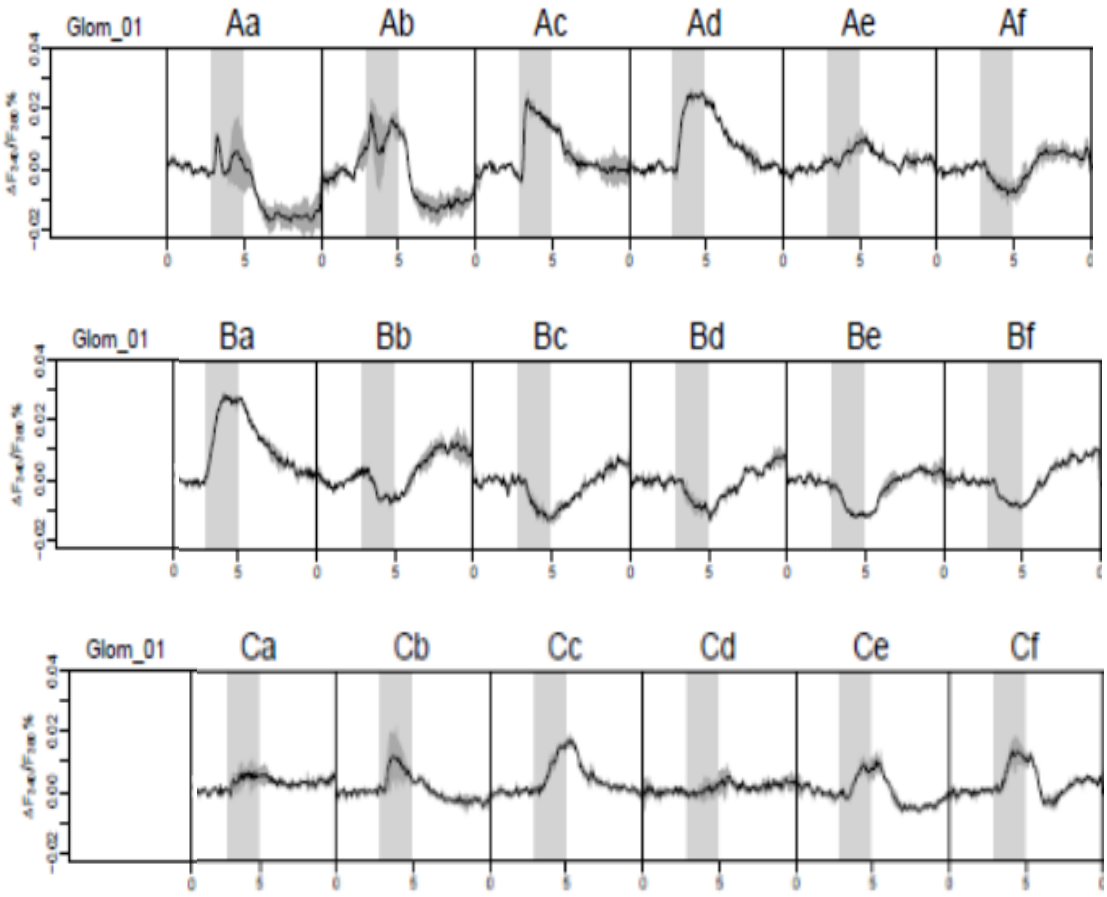

Figure 15a. *Mean traces of cumulus responses in preparation 3 to the primary (upper), secondary (mid), and interspecific (bottom) components. The stimulus period is indicated by the gray column.*

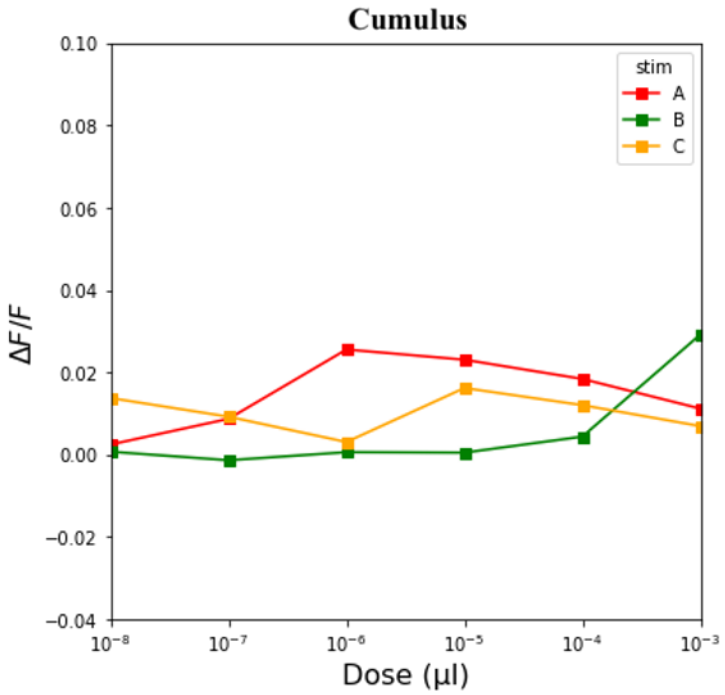

Figure 15b. *Dose response curves demonstrating cumulus responses in preparation 3. The red line named "A" indicates responses to the primary pheromone component, the green line named "B" demonstrates secondary pheromone component responses, and the yellow line named "C" indicates responses to the interspecific component.*

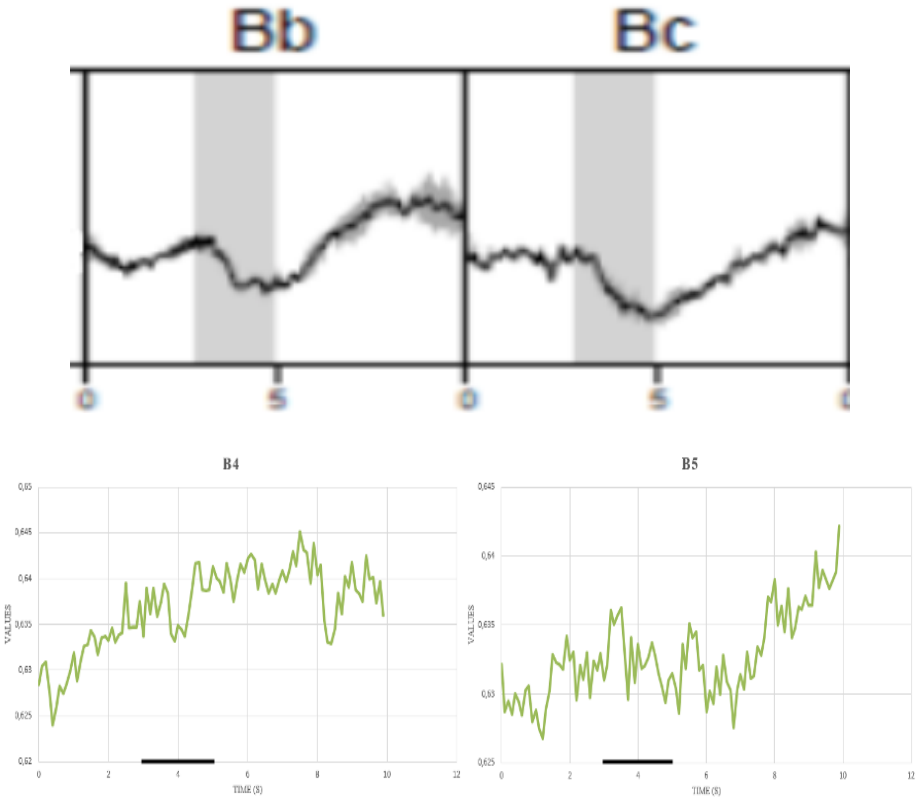

Figure 15c. *Comparison of mean traces and raw data traces in cumulus in preparation 3. The elevated black line in the raw data traces indicate the stimulation period from second 3 to 5.*

3.3.2 DMP Responses. When stimulated with the secondary pheromone component, B, a strong response was demonstrated by the highest concentration. No responses were elicited by the other concentrations of component B. The interspecific component, C, displayed weak activation with an exception of concentration 10^{-8}. The DMP was activated by concentrations 10^{-3}-10^{-4} and 10^{-6} of the primary pheromone component, A. The mean traces of all stimuli are shown in figure 16a, while figure 16b pictures the dose response relationship.

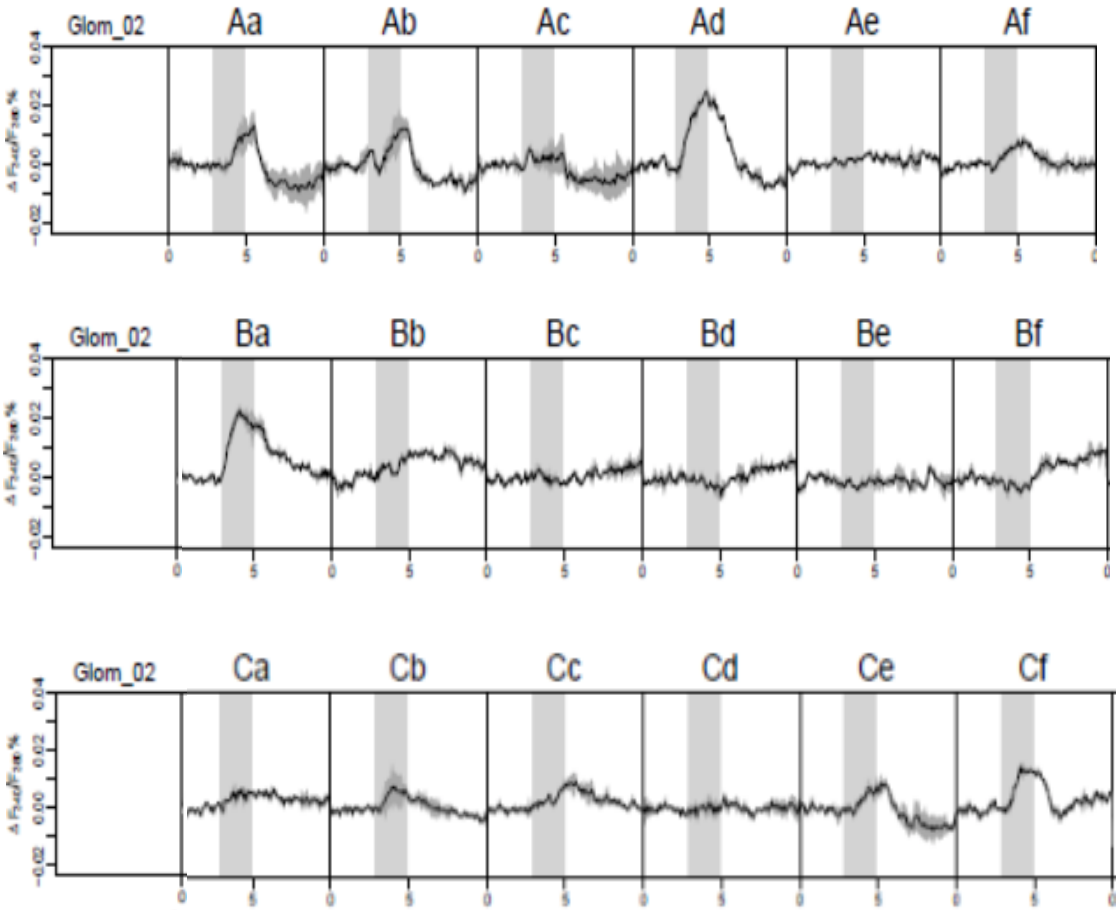

Figure 16a. *Mean traces of DMP responses in preparation 3 to the primary (upper), secondary (mid), and interspecific (bottom) components. The stimulus period is indicated by the gray column.*

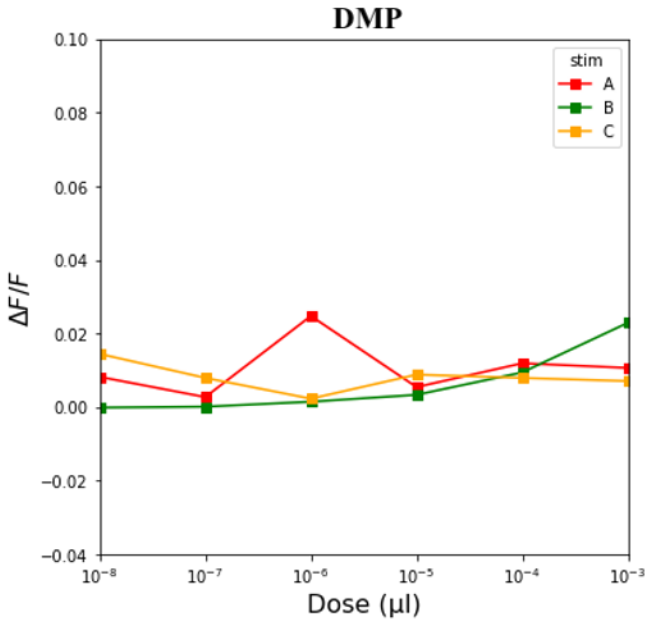

Figure 16b. *Dose response curves demonstrating DMP responses in preparation 3. The red line named "A" indicates responses to the primary pheromone component, the green line named "B" demonstrates secondary pheromone component responses, and the yellow line named "C" indicates responses to the interspecific component.*

3.3.3 DMA Responses. Little to no activation in the DMA was demonstrated during stimulation with most of the concentrations of the interspecific component, C. Concentration 10^{-4} elicited the most prominent response. When stimulated with the secondary pheromone component, B, a strong response was observed to the concentration 10^{-3} exclusively. During stimulation with the primary pheromone component, A, little activation was demonstrated, with the concentration 10^{-6} eliciting the strongest response. Figure 17a pictures the mean traces of all stimuli, while the dose response relationship is shown in figure 17b.

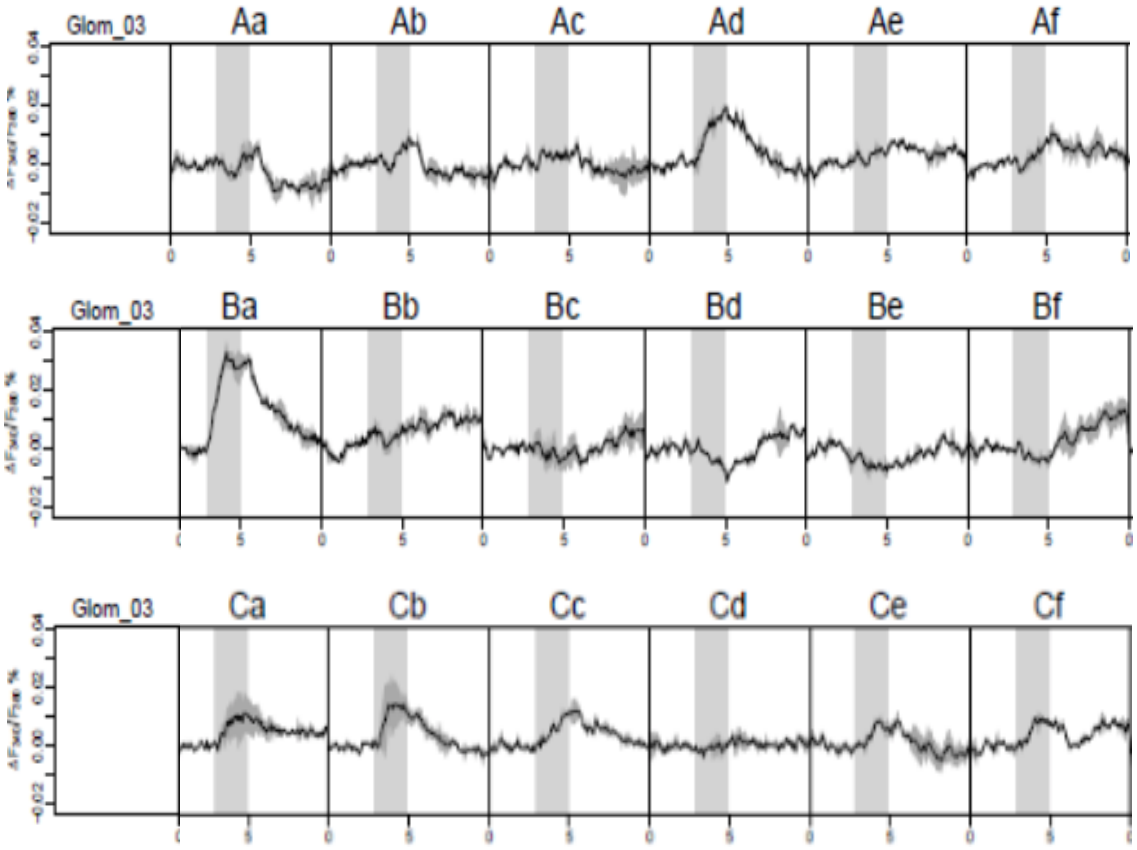

Figure 17a. *Mean traces of DMA responses in preparation 3 to the primary (upper), secondary (mid), and interspecific (bottom) components. The stimulus period is indicated by the gray column.*

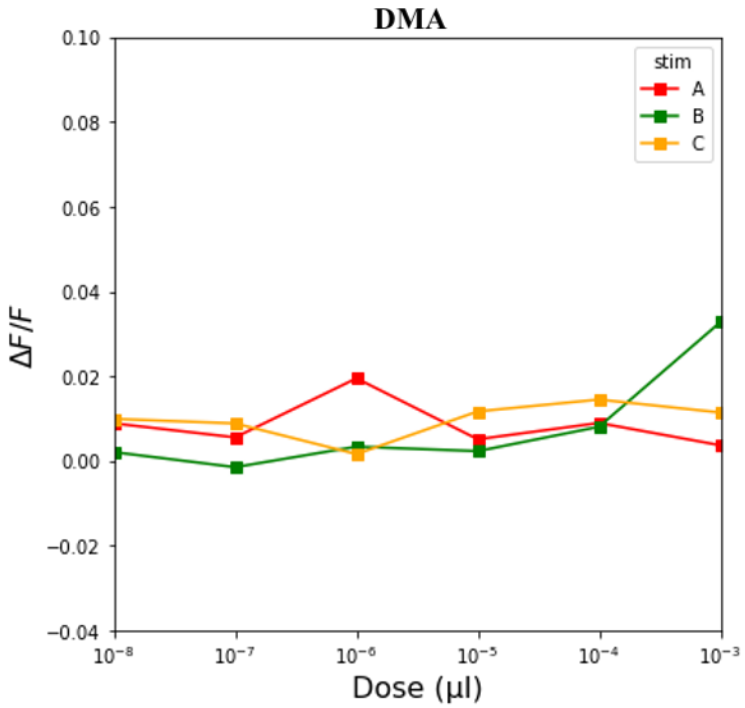

Figure 17b. *Dose response curves demonstrating DMA responses in preparation 3. The red line named "A" indicates responses to the primary pheromone component, the green line named "B" demonstrates secondary pheromone component responses, and the yellow line named "C" indicates responses to the interspecific component.*

3.4 Comparison of Responses Across Preparations

Cumulus in all three preparations elicited responses to high concentrations, 10^{-3}-10^{-6}, of the primary pheromone component, A. In addition, responses to the highest concentration, 10^{-3}, of the secondary pheromone component, B, was observed in preparation 2 and 3. Additionally, the lower concentrations seemed to elicit slight inhibitory responses. In terms of the interspecific component, C, different responses were observed across the three preparations. In preparation 1, concentration 10^{-3}, elicited a notable response, while preparation 3 demonstrated responses to 10^{-4}-10^{-5} and 10^{-7} and 10^{-8}, respectively. Preparation 2 showed no prominent responses to any concentrations of component C.

DMP responses to the highest concentration, 10^{-3}, of the secondary pheromone component, B, was observed across all three preparations. Preparation 1 and 2 also displayed responses to high concentrations, 10^{-3}-10^{-5}, of the interspecific component, C, while preparation 3 only displayed a slight excitatory response to concentration 10^{-8} of this

component. As for responses to the primary pheromone component, A, preparation 1 and 3 showed responses to various concentrations, 10^{-3}-10^{-4} and 10^{-3} and 10^{-6}, respectively. Preparation 2 showed no activation during component A stimulation.

In the DMA, all three preparations displayed moderate to high responses to the interspecific component, C. Regarding the secondary component, B, preparation 3 responded strongly to the highest concentrations, whereas preparation 1 and 2 displayed no to moderate responses to this compound. During stimulation with the primary pheromone component, A, preparation 1 demonstrated responses to the highest concentrations, 10^{-3}-10^{-4}, while preparation 3 only showed activation by concentration 10^{-6}. Interestingly, preparation 2 displayed slight inhibition.

4. Discussion

The present calcium-imaging study was a pilot project initiated to test MGC responses during stimulation with three relevant odor components, two pheromones and one interspecific component. This was done in order to identify the optimal substance concentration for calcium imaging studies. Certain limitations were identified with the analysis program KNIME, which was further considered throughout the project. I succeeded in completing the full experimental procedure in several preparations.

4.1 The Effect of Different Concentrations

Concentrations ranging from 10^{-3} to 10^{-8} were used in this project with the aim to identify the most favorable concentration for calcium imaging technique. Traditionally, very high concentrations, usually around 10^{-2}, have been used in calcium imaging studies (e.g. Skiri et al., 2004). This project demonstrates that such high concentrations are not necessary for providing strong signals.

Although there are three data sets which were presented in the results, only the first preparation demonstrated the good quality signals corresponding to the expected MGC units' responses. Unfortunately, the two other preparations demonstrated inconsistent and irrelevant for the further analysis responses due to the methodological complications described below.

Nevertheless, the first preparation gives us opportunity to validate the most relevant concentrations for the application in calcium imaging technique. Thus, for the cumulus activation, concentrations 10^{-3} and 10^{-4} are most effective for the primary pheromone component. It is important to notice that the interspecific component activates the cumulus at concentration of 10^{-3}, but very little on 10^{-4}, which means that the 10^{-4} is more favorable if we want to avoid the irrelevant activity of the cumulus to the interspecific component.

Further, the DMP unit showed responses to secondary pheromone and interspecific component at concentrations 10^{-3} and 10^{-4}, meaning that the 10^{-4} is high enough to elicit strong signals in the DMP. Interestingly, the interspecific component at 10^{-5} elicited higher responses demonstrating high sensitivity of the DMP projection neurons to the interspecific component.

The DMA unit showed strong responses to the interspecific component at concentration of 10^{-3} and to the primary pheromone at concentration of 10^{-3} and 10^{-4}. The DMA primary role is the processing of interspecific component, therefore the responses of this unit to the primary pheromone seems to be not corresponding to the naturally occurring events in the AL. Therefore, for the future calcium imaging studies to avoid the irrelevant activity of the DMA to the primary pheromone, concentration 10^{-5} should be used.

Considering the fact that different concentrations of the same compound can create different behavioral responses in the male moth, it is hard to identify a collectively favorable concentration across three MGC subunits. However, based on the data presented above, it is likely that concentration 10^{-5} is optimal for calcium imaging of the DMP and DMA, while concentration 10^{-4} is possibly more favorable for imaging of the cumulus.

4.2 Functional Characterization of the MGC Subunits

When applied to the antenna, every component elicited a distinct response pattern in the MGC. The cumulus demonstrated, as anticipated, responses to the primary pheromone, Z11-16:Ald, in all three preparations. In addition, responses to higher concentrations of both the secondary pheromone, Z9-16:Ald, and the interspecific component, Z9-14:Ald, were observed. The DMP was activated by Z9-16:Ald, but also showed some responses to Z11-16:Ald and Z9-14:Ald, across the preparations. Lastly, the DMA elicited the strongest response to the interspecific component, C, but various responses to the primary pheromone,

A and the secondary pheromone, B, across the preparations were also observed. Each of the MGC subareas will be further discussed in the following subsections.

4.2.1 Odor-Evoked Responses in the Cumulus. The results from this project demonstrated a cumulus response to Z11-16:Ald, in all preparations. The concentration eliciting the strongest activation was in the range of 10^{-4} and 10^{-5}. Previous research (e.g. Xu et al., 2016; Wu et al., 2015) have demonstrated support for the assumption that the cumulus is activated by Z11-16:Ald exclusively. However, these calcium-imaging bath application studies investigated primarily input neurons to the cumulus, while this project deals with the MGC output neurons. Nevertheless, this indicates a high consensus between AL input and output. The findings presented here are also in correspondence with former electrophysiological studies reporting about cumulus projection neurons responding to Z11-16:Ald (Vickers et al., 1998; Zhao & Berg, 2010; Christensen et al., 1991).

Although the results from this study is in line with previous findings including prominent cumulus responses to Z11-16:Ald, activation is also observed during stimulation with the two other components. Notably, these responses vary greatly between preparations and is significantly weaker than that of the primary pheromone component. As explained earlier in the text, the naturally occurring attractant in the *H. armigera* is a blend of Z11-16:Ald and Z9-16:Ald. It then makes sense that the unit responsible for processing the primary component is also sensitive to the secondary component, as they naturally occur together. However, the secondary component seems to elicit excitatory responses during the highest concentration (10^{-3}), but inhibitory effects when stimulated with the lower (10^{-5}-10^{-8}). Why this response pattern is occurring is not known. Additionally, various concentrations of the interspecific component Z9-14:Ald elicit responses across preparations, which is surprising due to its antagonistic characteristics in *H. armigera*. It is difficult to say why these responses are occurring, but it is possible that LN connections between the MGC glomeruli play a role here. Furthermore, the most probable reason for cross experimental differences is incorrect identification of the MGC units and unstable signals due to preparation movement.

4.2.2 Odor-Evoked Responses in DMP. The DMP demonstrates a predicted response to the secondary pheromone component Z9-16:Ald. Most prominent was the highest concentration (10^{-3}), but activation was also observed by 10^{-4} in at least one preparation.

Additionally, quite prominent responses were observed during stimulation with the interspecific component Z9-14:Ald, with the DMP in the various preparations appearing to respond strongly to this component. Even though responses to both Z9-16:Ald and Z9-14:Ald were expected and is in correspondence with previous findings (e.g. Xu et al., 2016; Wu et al., 2015), higher sensitivity to the Z9-16:Ald component was anticipated. This is very interesting considering the fact that the components have opposite behavioral effects. One possible explanation could be the weak-shape theory, which states that ORs strongly activated by a specific odor could show responses to an odor with a similar molecular shape (Jortner, 2013).

Responses to the primary pheromone component Z11-16:Ald, vary widely, with preparation 2 showing no response regardless of concentration, preparation 1 showing a response to concentrations 10^{-3} and 10^{-4}, and preparation 2 demonstrating a strong response to concentration 10^{-6}. Even though in preparation 1 calcium signals were significantly weaker, activation of the DMP in response to Z11-16:Ald stimulation was still surprising. This could possibly be due to the same mechanisms thought to modulate the equivalent pattern in the cumulus, with LN connectivity between the two MGC subunits. Since blend specificity is so crucial for precise communication between the Heliothinae subfamilies (reviewed by Berg et al., 2014), it is conceivable that a heightened sensitivity to the species-specific ratio is present.

4.2.3 Odor-Evoked Responses in DMA. The results from the DMA demonstrate inconsistencies across preparations. While preparation 1 displays prominent responses to the interspecific component Z9-14:Ald, as predicted, the responses observed in the two other preparations, are less apparent. However, activation of the DMA by the interspecific component is in line with previous research (e.g. Xu et al., 2016; Wu et al., 2015). Furthermore, high concentrations of Z9-16:Ald show activation in preparation 2 and 3, while preparation 1 shows no obvious response. Surprisingly, Z11-16:Ald shows quite strong responses in preparation 1 and essentially no response in the two other preparations. With a variety across preparations it is hard to determine actual effects. It is conceivable that the preparations' movement in the course of calcium imaging leads to incorrect recognition of the glomeruli in KNIME and consequently incorrect correspondence between a glomerulus and time traces.

An interesting fact here is the DMA activation by primary pheromone Z11-16:Ald. Since the interspecific component and primary pheromone have opposite behavioral effects in

the *H. armigera*, it is important for the male to be able to make a clear distinction between them. Wrongly interpreting these signals could result in interspecific mating. The sensitivity for these components is therefore most likely heightened. Interestingly, previous findings demonstrate an inhibitory effect in neurons tuned to the interspecific component when stimulated with the primary pheromone (Zhao & Berg, 2010), an opposite effect of what has been observed in this project. However, the model organism used in that study was the closely related species *H. assulta*, which differs slightly from the *H. armigera* in its MGC organization. Even though the species are closely related, there might be some underlying differences regarding signal coding.

4.3 Methodological Considerations

4.3.1 Calcium Imaging. Calcium imaging is a great method for investigation of neurons on a neuronal population level. The method allows for a relatively long stimulus list, making it an appropriate recording method for MGC sensitivity to various concentrations. However, as with *in vivo* methods, several challenges are present.

Movement of a preparation in calcium imaging can be due to several factors, but the most prominent are muscle pumping and poor fixing of the preparation. By removing certain muscles in the brain, the pumping can be accounted for. However, the muscle in question has to be pulled out with forceps from underneath the AL which makes it hard to access in some preparations. When fixing the head with wax (*see section 2.2 Preparation in methods*) it is crucial to take your time and make sure it is completely immobilized. Even though KNIME possess a possibility for movement correction, too much of the motion can result in an inaccurate glomeruli recognition.

Since the MGC is located at the entrance of the antennal nerve, it can be difficult to get a clear image of it. In some preparations, cuticula surrounding the antennae partially covers the AL, making it hard to access the MGC. With caution you can remove it and provide a clearer view without damaging the nerve. Once ready for imaging, the correct focal plan has to be found. Focusing too deep provides a blurry image, while too superficial make it hard to identify and record glomeruli responses. In some cases, it is difficult to identify the correct focal plan before data processing. Usually, it is based on an educated guess and experience where the MGC and ordinary glomeruli are clearly visible.

To some extent, *in vivo* recordings will always produce some signal noise, which is the combinatory result of the beforehand mentioned factors (Reviewed by Christensen & Nedergaard, 2011). Preferably, the signal-to-noise ratio would be strong signal to low noise, but in calcium imaging this can be hard to achieve. Additionally, nervous tissue is very sensitive to photodamage, especially in the presence of fluorophores. When exposed to light, fluorophores generate free radicals resulting in cell damage and bleaching (Stephens & Allan, 2003). Nevertheless, these challenges were kept in mind throughout the experimental process. When executed correctly, calcium imaging can provide valuable insight difficult to acquire by the use of other methods, like providing information about activity in numerous neurons at the same time. While some of the challenges are easily solvable, others, like bleaching, are more difficult to confront. However, radiometric dyes like Fura-2 dextran diminish such problems to some extent. In the end, every experimental method has advantages and disadvantages, the key is to be aware of them while conducting experiments.

4.3.2 Analysis. Analyzing raw data by the use of KNIME has the advantages that it can create a clear overview of the AL glomeruli by generating a digital map. However, throughout this project, several disadvantages were identified with the KNIME program as well. Although KNIME initially is a great tool for processing of this type of raw data, some concerns were raised during the further and final processing.

For some preparations with high degree of movement during imaging, preliminary analysis of the data showed that the MGC units did not match the expected response profile known from previous studies. Therefore, the comparison between raw data and processed data in KNIME and RStudio were performed. Several inconsistencies between the raw data and the processed data were observed. All of the problems identified with KNIME most likely relate to movement, and KNIME not being able to correct for it in an adequate manner. A peculiar response pattern was identified in preparation 2 during stimulation with Z9-16:Ald, concentration 10^{-4}. The difference between the two trials were obvious (*see figure 12a*) and must be due to great movement. However, comparing the raw data traces and the processed traces displayed little difference between them. Nevertheless, this raises a question regarding the accuracy of the remaining data. Is the cumulus, DMA and DMP recognized by KNIME in fact the authentic MGC subunits, or did movement distort the AL map providing biased results?

Looking though the raw data for preparation 3 a shifting movement throughout the entire trial were identified, raising the same question as for preparation 2. KNIME´s insufficient correcting of movement could result in, for example, identification of two glomeruli as one, creating a biased output for further processing in R and Python. There is possible that the big variation seen between trials could be due to this kind of instability. Additionally, as mentioned above, differences in response patterns were observed across the preparations, which were not in compliance with previously reported findings. It is conceivable that this is at least partially due to the same issues.

Further, when comparing single raw data traces with the processed data traces some responses displayed little consensus. As seen in figure 14c, raw data traces for DMA responses to Z11-16:Ald, display quite prominent responses, while the processed traces demonstrate no response. Additionally, figure 15c presents different response patterns in cumulus for Z9-16:Ald, which makes it quite certain that something happened to the data on the journey from raw data to finished, processed data. Awareness and identification of limitations or disadvantages is crucial for further development within a research field.

4.4 Further Investigations

Despite several challenges, this project demonstrates that it is not trivial to perform experiments for obtaining a dose response relationship with help from calcium imaging. A dose response curve was supposed to be achieved but proved to be difficult to obtain (due to beforehand mentioned uncertainties) in contrast with the dose response relationship for OSNs from previous studies (e.g. Berg & Mustaparta, 1995). The sub-goals of identifying the lowest detectable concentration and the highest concentration before reaching saturation were therefore hard to obtain. The main reason for this is the fact that calcium signals are not consistent depending much on experimental performance and signal stability.

Among the datasets presented, preparation 1 shows the most relevant and expected results. From a statistical perspective, three datasets are not sufficient to make any conclusions. Furthermore, the data for the last two preparations are not suitable for including into statistical analysis due to inadequate data quality. These datasets are only included in the results as part of the work. For further investigations, similar experiments should be conducted including more good signal preparations.

Nevertheless, the main outcome from the present project is to prove that the previously used concentrations were too high, being not biologically relevant and therefore not beneficial for this type of experiments. Future research should therefore use lower concentrations, like the ones identified in this project.

Lastly, LNs have been mentioned in this discussion a considerable amount of times, but the exact functionality of these neurons and how they affect MGC activation patterns are uncertain. Further insight into the modulatory role of the LNs and the interaction between the MGC glomeruli would be highly beneficial for the research field. Furthermore, as previously mentioned, there is a possibility that the ambiguous activation patterns observed in the results are due to methodological limitations. Further identification of challenges related to methods and how to resolve these, should therefore be a priority, which in the long run could strengthen this type off research methodologically. Overall, the results demonstrate quite big discrepancies between certain traces, providing biased results. In this project, these weaknesses were identified, future research should put emphasis on how to resolve them.

5. Conclusion

Successfully performed retrograde staining of the PNs confined to the mALT made it possible to measure odor-evoked responses in the MGC to different concentrations of two pheromone components and one interspecific component by the use of calcium imaging.

Despite inconsistencies of the results, the concentrations 10^{-4} and 10^{-5} was identified as the most beneficial concentration for calcium imaging studies. These concentrations are lower than the concentration frequently used previously (10^{-2}), demonstrating that the latter one is unjustifiably high. To avoid glomeruli activation by irrelevant stimuli, differential approach by using distinct concentrations for different components could be taken into consideration. However, considering the small size of the obtained data, more research should be done to strengthen this assumption and to define optimal concentration for each of the components used in calcium imaging.

References

Anton, S. & Homberg, U. (1999). Antennal Lobe Structure. In Hansson, B. S. (Ed.), *Insect Olfaction* (97-124). Springer.

Berg, B. G. & Mustaparta, H. (1995). The Significance of Major Pheromone Components and Interspecific Signals as Expressed by Receptor Neurons in the Oriental Tobacco Budworm Moth, *Helicoverpa assulta*. *Journal of Comparative Physiology, 177*(6), 683-694. 10.1007/BF00187627

Berg, B. G., Schachtner, J. & Homberg, U. (2009). γ-Aminobutyric Acid Immunostaining in the Antennal Lobe of the Moth *Heliothis virescens* and its Colocalization with Neuropeptides. *Cell and Tissue Research, 335*(3), 593-605. 10.1007/s00441-008-0744-z

Berg, B. G., Tumlinson, J. H. & Mustaparta, H. (1995). Chemical Communication in Heliothine Moths. *Journal of Comparative Physiology, 177*(5), 527-534. 10.1007/BF00207182

Berg, B. G., Zhao, X. C. & Wang, G. (2014). Processing of Pheromone Information in Related Species of Heliothine Moths. *Insects, 5*(4), 742-761. 10.3390/insects5040742

Berridge, M. J., Lipp, P. & Bootman, M. D. (2000). The Versatility and Universality of Calcium Imaging. *Molecular Cell Biology, 1*(1), 11-21. 10.1038/35036035

Butenandt, A. (1959). Wirkstoffe des Insektenreiches. *Naturwissenschaften, 46*(15), 461-471. 10.1007/BF00634039

Chang, H., Mengbo, G., Wang, B., Lui, Y., Dong, S. & Wang, G. (2016). Sensillar Expression and Responses of Olfactory Receptors Reveal Different Peripheral Coding in Two *Helicoverpa* Species Using the Same Pheromone Components. *Scientific*

Reports, 6(1), 1-12. 10.1038/srep18742

Christensen, D. J. & Nedergaard, M. (2011). Two Photon in Vivo Imaging of Cells. *Pediatric Nephrology, 26*(9), 1483-1489. 10.1007/s00467-011-1818-9

Christensen, T. A., Mustaparta, H. & Hildebrand, J. G. (1991). Chemical Communication in Heliothine Moths. *Journal of Comparative Physiology, 169*(3), 259-274. 10.1007/BF00206990

Christensen, T. A. & Hildebrand, J. G. (1987). Male-Specific, Sex Pheromone-Selective Projection Neurons in the Antennal Lobes of the Moth *Manduca sexta*. *Journal of Comparative Physiology, 160*(5), 553-569. 10.1007/BF00611929

Christensen, T. A. & Hildebrand, J. G. (2002). Pheromonal and Host-odor Processing in the Insect Antennal Lobe: How Different? *Current Opinion in Neurobiology, 12*(4), 393-399. 10.1016/S0959-4388(02)00336-7

Christensen, T. A., Waldrop, B. R., Harrow, I. D. & Hildebrand, J. G. (1993). Local Interneurons and Information Processing in the Olfactory Glomeruli of the Moth *Manduca sexta*. *Journal of Comparative Physiology, 173*(4), 385-399.

Dacks, A. M., Christensen, T. A., Agricola, H. J., Wollweber, L. & Hildebrand, J, G. (2005). Octopamine-Immunoreactive Neurons in the Brain and Subesophageal Ganglion of the Hawkmoth *Manduca sexta*. *Journal of Comparative Neurology, 488*(3), 255-268. 10.1002/cne.20556

Dacks, A. M., Christensen, T. A. & Hildebrand, J. G. (2006). Phylogeny of a Serotonin Immunoreactive Neuron in the Primary Olfactory Center of the Insect Brain. *Journal of Comparative Neurology, 498*(6), 727-746. 10.1002/cne.21076

Deisig, N., Dupuy, F., Anton, S. & Renou, M. (2014). Responses to Pheromones in a Complex Odor World: Sensory Processing and Behavior. *Insects, 5*(2), 399-422.

10.3390/insects5020399

Diongue, A., Yang, J. T. & Lai, P. Y. (2013). Biomorphometric Characteristics of Different Types of Sensilla Detected on the Antennae of *Helicoverpa armigera* by Scanning Electron Microscopy. *Journal of Asia-Pacific Entomology, 16*(1), 23-28. 10.1016/j.aspen.2012.09.001

Fişek, M. & Wilson, R. I. (2014). Stereotyped Connectivity and Computations in Higher Order Olfactory Neurons. *Nature Neuroscience, 17*(2), 280-288. Doi: 10.1038/nn.3613

Galizia, G. C. & Rössler, W. (2010). Parallel Olfactory Systems in Insects: Anatomy and Function. *Annual Reviews of Entomology, 55*, 399-420. 10.1146/annurev-ento 112408-085442

Galizia, G. C., Sache, S. & Mustaparta, H. (2000). Calcium Responses to Pheromone and Plant Odors in the Antennal Lobe of the Male and Female Moth *Heliothis virescens*. *Journal of Comparative Physiology, 186*(11), 1049-1063. 10.1007/s003590000156

Gough, S. C. L., Belda-Iniesta, C., Poole, C., Weber, M., Russel-Jones, D., Hansen, F. B., Mannucci, E. & Tuomilehto, J. (2011). Insulin Therapy in Diabetes and Cancer Risk: Current Understanding and Implications for Future Study. *Advances in Therapy, 28*(5), 1-18. 10.1007/s12325-011-0047-8

Grienberger, C. & Konnerth, A. (2012). Imaging Calcium in Neurons. *Neurons, 73*(5), 862-885. 10.1016/j.neuron.2012.02.011

Hallem, E. A. & Carlson, J. R. (2006). Coding of Odors by a Receptor Repertoire. *Cell, 125*(1), 143-160. 10.1016/j.cell.2006.01.05

Helmchen, F. & Waters, J. (2002). Ca^{2+} Imaging in the Mammalian Brain in Vivo. *European Journal of Pharmacology, 447*(2), 119-129. 10.1016/S0014-2999(02)01836-8

Homberg, U., Montague, R. A. & Hildebrand, J. G. (1988). Anatomy of Antenno-Cerebral

Pathways in the brain of the Sphinx Moth *Manduca sexta*. *Cell and Tissue Research, 254*(2), 255-281. 10.1007/BF00225800

Ian, E., Berg, A., Lillevoll, S. C. & Berg, B. G. (2016[a]). Antennal-Lobe Tracts in the Noctuid Moth, *Heliothis virescens*: New Anatomical Findings. *Cell and Tissue Research, 366*(1), 23-35. 10.1007/s00441-016-2448-0

Ian, E., Kirkerud, N. H., Galizia, G. C. & Berg, B. G. (2017). Coincidence of Pheromone and Plant Odor Leads to Sensory Plasticity in the Heliothine Olfactory System. *PloS One, 12*(5), 1-16. 10.1371/journal.pone.0175513

Ian, E., Zhao, X. C., Lande, A. & Berg, B. G. (2016[b]). Individual Neurons Confined to Distinct Antennal-Lobe Tracts in the Heliothine Moth: Morphological Characteristics and Global Projection Patterns. *Frontiers in Neuroanatomy, 10*(101), 1-19. 10.3389/fnana.2016.00101

Jortner, R. A. (2013). Neural Coding in the Olfactory System. In Quian Quiroga, R. & Panzeri, S. (Eds.), *Principles of Neural Coding* (225-262). Taylor & Francis.

Karlson, P. & Luscher, M. (1959). Pheromones: A New Term for a Class of Biologically Active Substances. *Nature, 183*(4653), 55-56. 10.1038/183055a0

Kehat, M., Gothilf, S., Dunkelblum, E. & Greenberg, S. (1980). Field Evaluation of Female Sex Pheromone Components of the Cotton Bollworm, *Heliothis armigera*. *Entomologia Experimentalis et Applicata, 27*(2), 188-193. 10.1111/j.1570 7458.1980.tb02963.x

Laurent, G. & Naraghi, M. (1994). Odorant-Induced Oscillations in the Mushroom Bodies of the Locust. *The Journal of Neuroscience, 14*(5), 2993-3004. 10.1523/JNEUROSCI.14-05-02993.1994

Martin, J. P., Beyerlein, A., Dacks, A. M., Reisenman, C. E., Riffell, J. A., Lei, H. &

Hildebrand, J. G. (2011). The Neurobiology of Insect Olfaction: Sensory Processing in a Comparative Context. *Progress in Neurobiology, 95*(3), 427-447. https://doi.org/10.1016/j.pneurobio.2011.09.007

Moffett, D. B., El-Masri, H. A. & Fowler, B. A. (2007). General Considerations of Dose Effect and Dose-Response Relationships. In Nordberg, G. F., Fowler, B. A., Nordberg, M. & Friberg, L. (Red.), *Handbook on the Toxicology of Metals* (3rd edition, p.101 115). Elsevier.

Murthy, M., Fiete, I. & Laurent, G. (2008). Testing Odor Response Stereotypy in the *Drosophila* Mushroom Body. *Neuron, 59*(6), 1009-1023. https://doi.org/10.1016/j.neuron.2008.07.040

Mustaparta, H. (1996). Central Mechanisms of Pheromone Information Processing. *Chemical Senses, 21*(2), 269-275. https://doi.org/10.1093/chemse/21.2.269

Patlak, M. (2003). Insect Pheromones: Mastering Communication to Control Pests. *National Academy of Sciences*, 1-9. http://www.nasonline.org/publications/beyond-discovery/insect-pheromones.pdf

Rollmann, S. M., Wang, P., Date, P., West, S. A., Mackay, T. F. C. & Anholt, R. R. H. (2010). Odorant Receptor Polymorphisms and Natural Variation in Olfactory Behavior in *Drosophila melanogaster*. *Genetics, 186*(), 687-697. 10.1534/genetics.110.119446

Sato, K., Pellegrino, M., Nakagawa, T., Nakagawa, T., Vosshall, L. B. & Touhara, K. (2008). Insect Olfactory Receptors are Heteromeric Ligand-Gated Ion Channels. *Nature, 452*(7190), 1002-1006. 10.1038/nature06850

Schultzhaus, J. N., Saleem, S., Iftikhar, H. & Carney, G. E. (2017). The Role of the Drosophila Lateral Horn in Olfactory Information Processing and Behavioral

Response. *Journal of Insect Physiology, 98*, 29-37. http://dx.doi.org/10.1016/j.jinsphys.2016.11.007

Skiri, H. T., Galizia, C. G. & Mustaparta, H. (2004). Representation of Primary Plant Odorants in the Antennal Lobe of the Moth *Heliothis virescens* Using Calcium Imaging. *Chemical Senses, 29*(3), 253-267. 10.1093/chemse/bjh026

Skiri, H. T., Rø, H., Berg, B. G. & Mustaparta, H. (2005). Consistent Organization of Glomeruli in the Antennal Lobes of Related Species of Heliothine Moths. *The Journal of Comparative Neurology, 491*(4), 367-380. 10.1002/cne.20692

Stephens, D. J. & Allan, V. J. (2003). Light Microscopy Techniques for Live Cell Imaging. *Science, 300*(5616), 82-86. 10.1126/science.1082160

Stopfer, M. (2014). Central Processing in the Mushroom Bodies. *Current Opinion in Insect Science, 6*, 99-103. 10.1016/j.cois.2014.10.009

Strauch, M., Rein, J., Lutz, C. & Galizia, G. C. (2013). Signal Extraction from Movies of Honeybee Brain Activity: The ImageBee Plugin for KNIME. *BMC Bioinformatics, 14*(18), 1-13. 10.1186/1471-2105-14-S18-S4

Tsien, R. Y. (1989). Fluorescent Probes of Cell Signaling. *Annual Reviews Neuroscience, 12*(1), 227-253. 10.1146/annurev.ne.12.030189.001303

Vickers, N. J., Christensen, T. A. & Hildebrand, J. G. (1998). Combinatorial Odor Discrimination in the Brain: Attractive and Antagonist Odor Blends are Represented in Distinct Combinations of Uniquely Identifiable Glomeruli. *The Journal of Comparative Neurology, 400*(1), 35-56. doi.org/10.1002/(SICI)10969861(19981012)400:1<35::AID-CNE3>3.0.CO;2U

Wu, H., Xu, M., Hou, M., Huang, L. Q., Dong, J. F. & Wang, C. Z. (2015). Specific Olfactory Neurons and Glomeruli are Associated to Differences in Behavioral Responses to

Pheromone Components between Two *Helicoverpa* Species. *Frontiers in Behavioral Neuroscience, 9*(206), 1-11. 10.3389/fnbeh.2015.00206

Xu, M., Guo, H., Hou, C., Wu, H., Huang, L. Q. & Wang, C. Z. (2016). Olfactory Perception and Behavioral Effects of Sex Pheromone Gland Components in *Helicoverpa armigera* and *Helicoverpa assulta*. *Scientific Reports, 6*(22998), 1-13. 10.1038/srep22998

Zhang, D. D. & Löfstedt, C. (2015). Moth Pheromone Receptors: Gene Sequences, Function, and Evolution. Frontiers in Ecology and Evolution, 3(105), 1-10. https://doi.org/10.3389/fevo.2015.00105

Zhang, J. P., Salcedo, C., Fang, Y. L., Zhang, R. J. & Zhang, Z. N. (2012). An Overlooked Component: (Z)-9-tetradecenal as a Sex Pheromone in *Helicoverpa Armigera*. *Journal of Insect Physiology, 58*(9), 1209-1216. 10.1016/j.jinsphys.2012.05.018

Zhao, X. C. & Berg, B. G. (2010). Arrangement of Output Information from the 3 Macroglomerular Units in the Heliothine Moth *Helicoverpa assulta*: Morphological and Physiological Features of Male-Specific Projection Neurons. *Chemical Senses, 35*(6), 511-521. 0.1093/chemse/bjq043

Zhao, X. C., Chen, Q. Y., Guo, P., Xie, G. Y., Tang, Q. B., Guo, X. R. & Berg, B. G. (2016). Glomerular Identification in the Antennal Lobe of the Male Moth *Helicoverpa armigera. The Journal of Comparative Neurology, 524*(15), 2993-3013. 10.1002/cne.24003

Zhao, X. C., Kvello, P., Løfaldli, B. B., Lillevoll, S. C., Mustaparta, H. & Berg, B. G. (2014). Representation of Pheromones, Interspecific Signals, and Plant Odors in Higher Olfactory Centers; Mapping Physiologically Identified Antennal-Lobe Projection Neurons in the Male Heliothine Moth. *Frontiers in Systems Neuroscience, 8*(186), 1-

14. 10.3389/fnsys.2014.00186

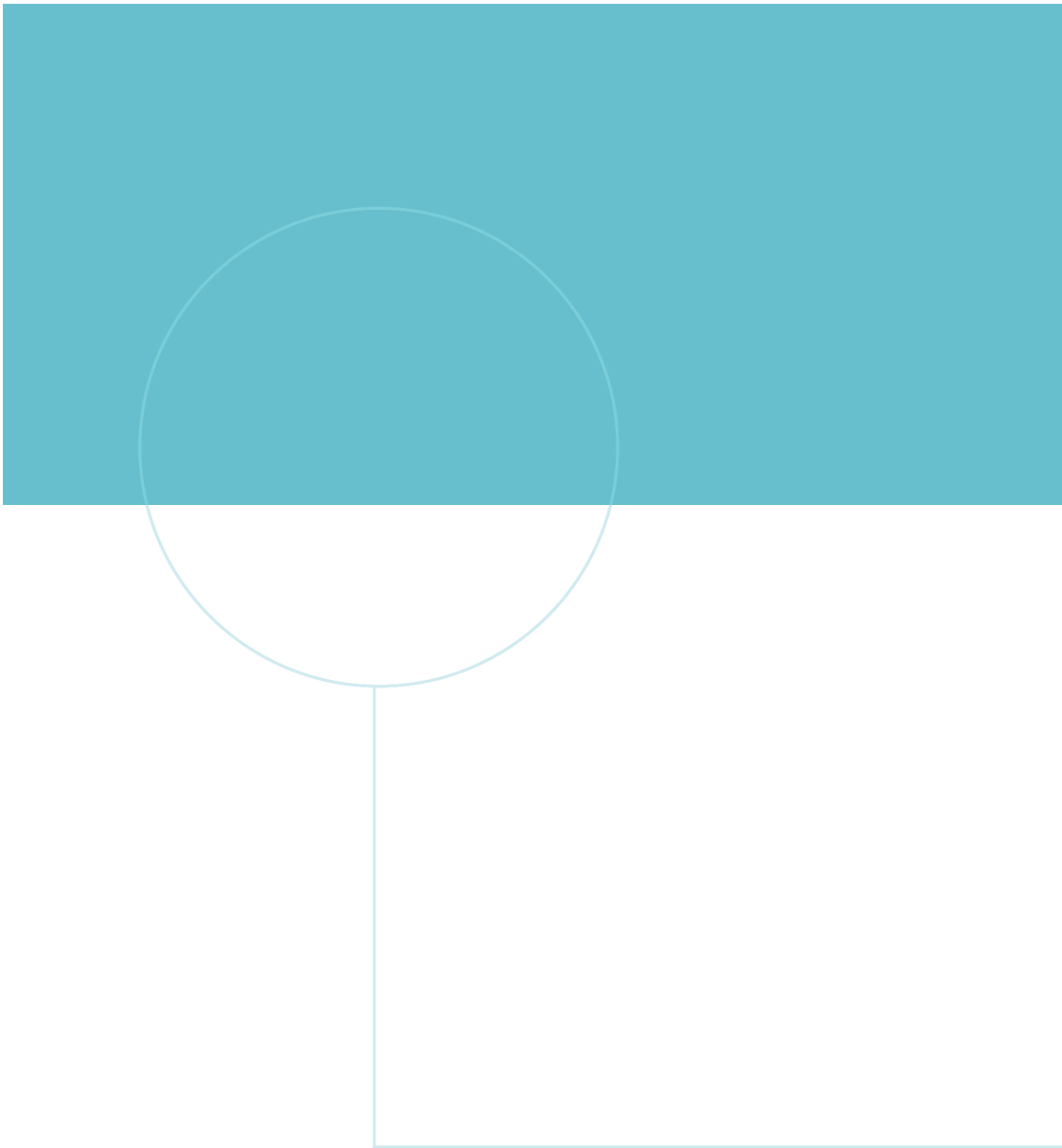

NTNU

Norwegian University of
Science and Technology